Modified Few-Body Faddeev-type Equations in Configuration Space

Renat A. Sultanov

The University of Texas Permian Basin

E. University Blvd., Odessa, TX 79764, USA

Pan-American Few-Body Physics Boot Camp: Fostering Collaboration

TRENTO, ITALY

October 13 - October 24, 2025

E-mail: sultanov_r@utpb.edu & r.sultanov2@yahoo.com *(private)*

Few-Body Systems and Few-Body Equations

- **Three-Body Problem:** In celestial mechanics, this problem raises the question of how to predict the trajectories of three interacting bodies, such as the Sun, Earth, and Moon.
- Henri Poincaré was the first to realize that the three-body problem is generally unsolvable.

Henri Poincaré

- **Isaac Newton in his 1687 book,** "The Mathematical Principles of Natural Philosophy", also explored the three-body problem.
- He successfully solved the motion of two celestial bodies under mutual gravity. However, he discovered that introducing a third body made the system fundamentally more complex and difficult to predict.

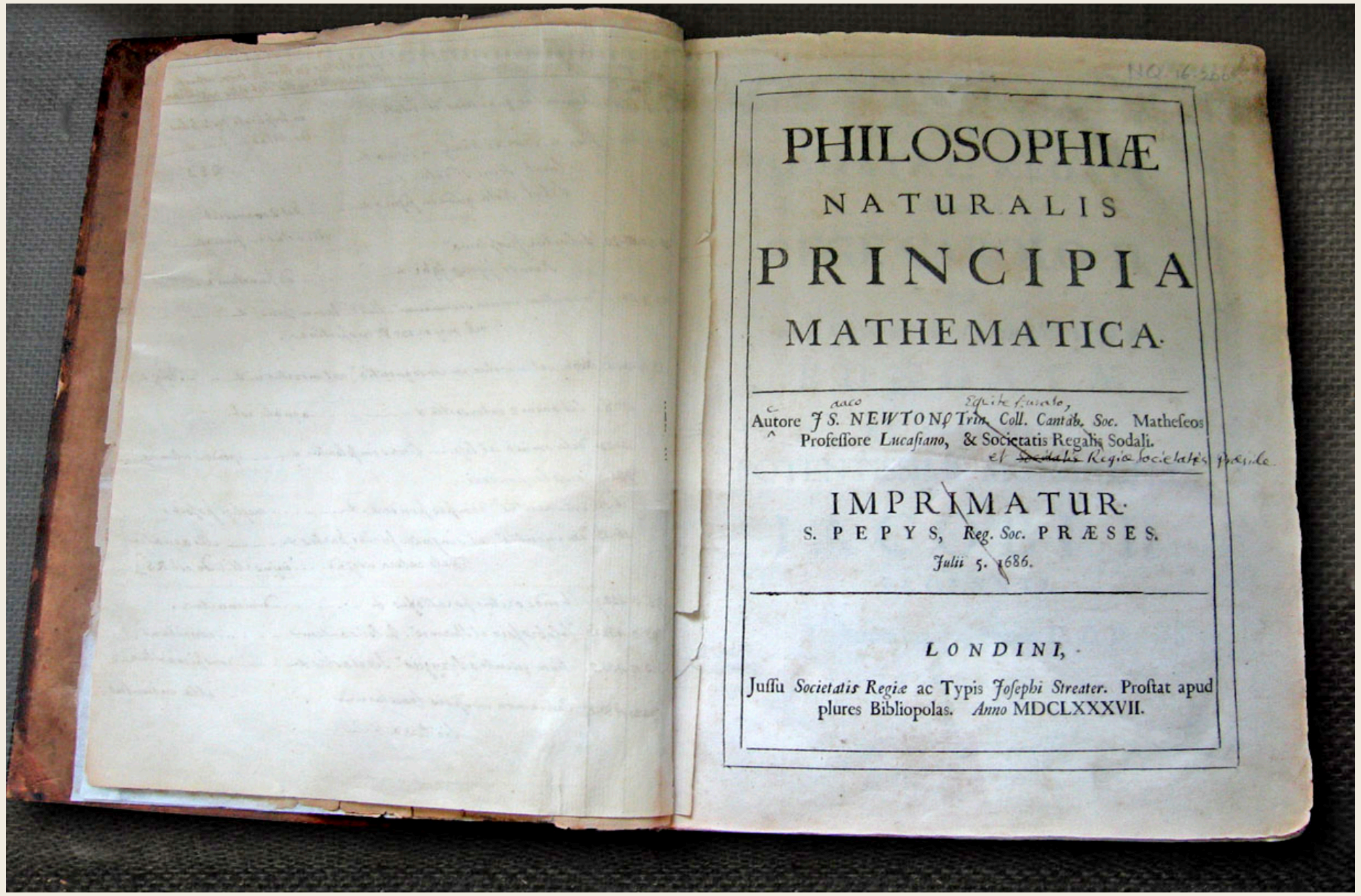

Isaac Newton

- The Faddeev equations are a quantum mechanical formulation that was proposed by Ludvig Faddeev in the 1960s for the purpose of solving the three-body scattering problem.

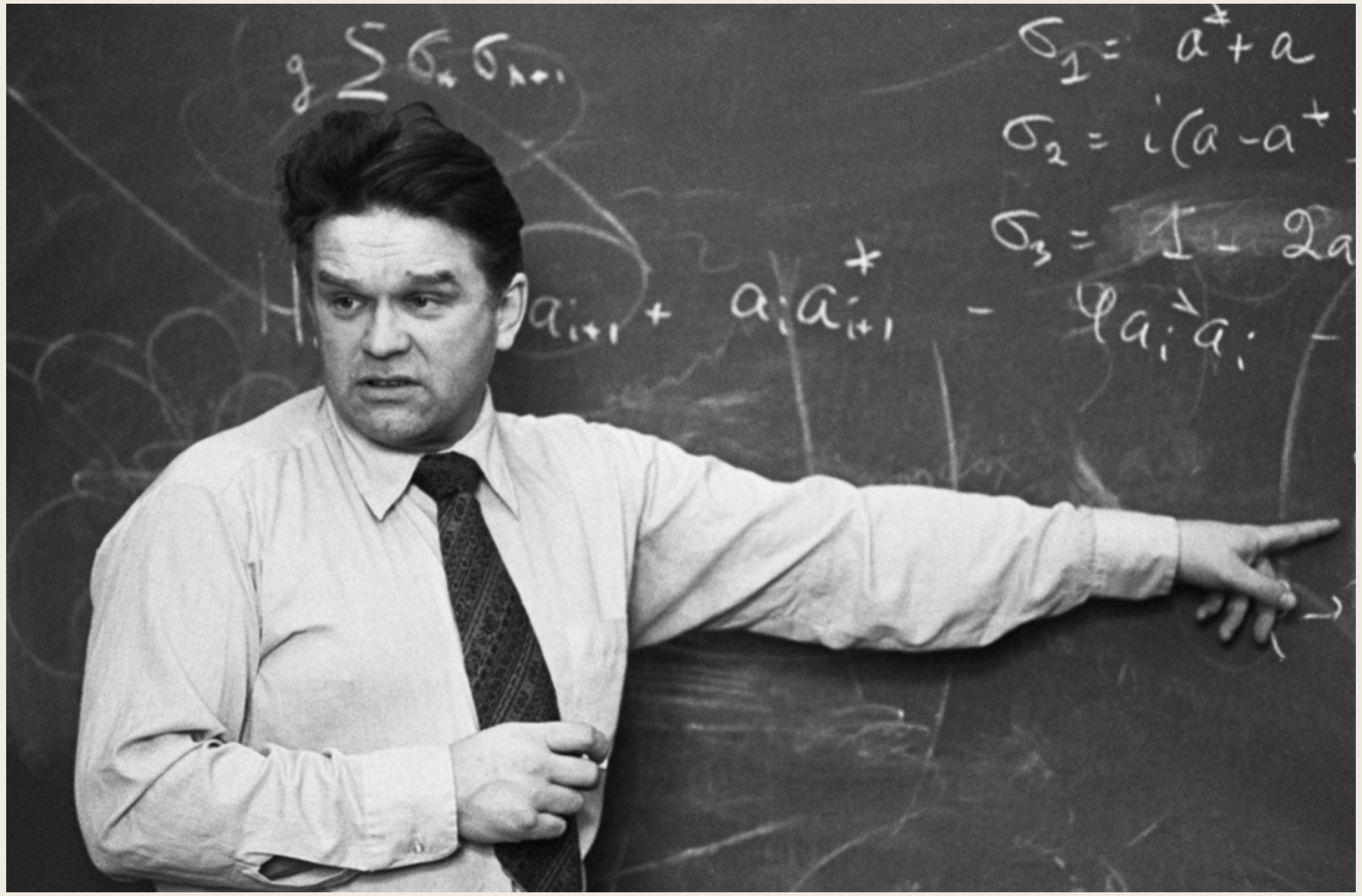

Ludvig Faddeev

1934-2017

- The AGS (Alt-Grassberger-Sandhas) equations are a type of Faddeev integral equation used in few-body physics to describe the scattering and binding energies of few-particle systems.
- This is achieved by reducing the problem to a set of coupled two-body Lippmann–Schwinger equations.

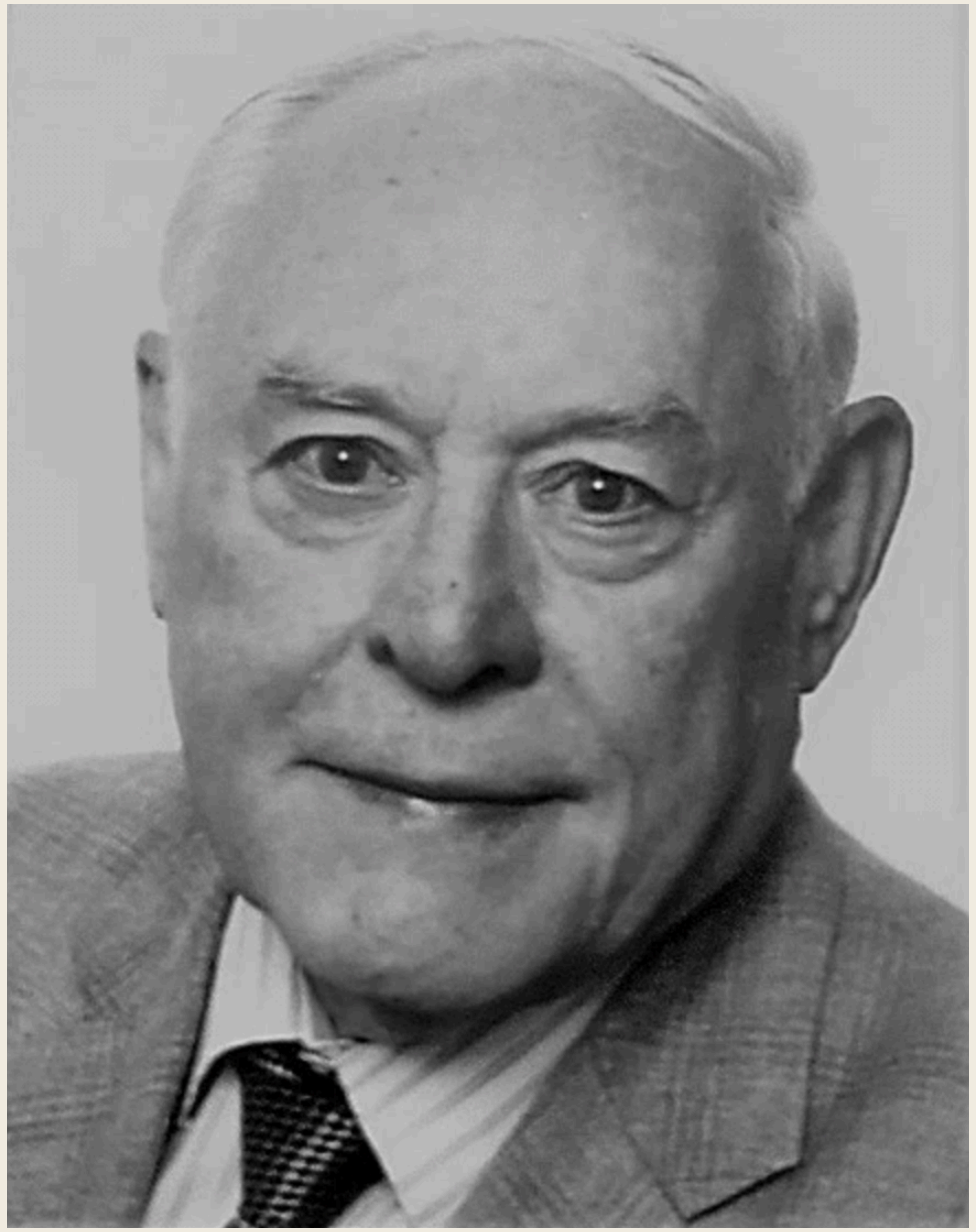

Detailed Few-Body Equations for Quantum Few-Body Systems

- L.D.Faddeev, Sov. Phys.-JETP 12, 1014 (1961).
- L.D.Faddeev, "Mathematical Aspects Of The Three Body Problem In The Quantum Scattering Theory", 1965 ISPT, Israel (English).
- E.O. Alt, P. Grassberger, W. Sandhas, Nucl. Phys. B 2, 167 (1967).
- Y. Hahn, Phys. Rev. 169, 794 (1968).
- W. Tobocman, Phys. Rev. C 9, 2466 (1974); 10, 60 (1974); 11, 43 (1975); 12, 741 (1975); 43 (1975).
- Y. Hahn and K. Watson, Phys. Rev. A 5, 1718 (1972).
- Y. Hahn, D. J. Kouri, and F. S. Levin, Phys. Rev. C 10, 1615 (1974).
- Y. Hahn, Phys. Rev. C 16, 2449 (1977).
- F. S. Levin, Phys. Rev. C 21, 2199 (1980).
- Y. Hahn, Phys. Lett. B 97, 1 (1980).
- Y. Hahn, Nucl. Phys. A 389, 1 (1982).

Three-body systems with *arbitrary masses*.

The total wave-function can be represented as:

$$|\Psi\rangle = \Psi_1(\mathbf{r}_{23}, \boldsymbol{\rho}_1) + \Psi_2(\mathbf{r}_{13}, \boldsymbol{\rho}_2),$$

$$\left(E - \hat{H}_0 - V_{23}(\mathbf{r}_{23})\right)\Psi_1(\mathbf{r}_{23}, \boldsymbol{\rho}_1) = \left(V_{23}(\mathbf{r}_{23}) + V_{12}(\mathbf{r}_{12})\right)\Psi_2(\mathbf{r}_{13}, \boldsymbol{\rho}_2),$$

$$\left(E - \hat{H}_0 - V_{13}(\mathbf{r}_{13})\right)\Psi_2(\mathbf{r}_{13}, \boldsymbol{\rho}_2) = \left(V_{13}(\mathbf{r}_{13}) + V_{12}(\mathbf{r}_{12})\right)\Psi_1(\mathbf{r}_{23}, \boldsymbol{\rho}_1).$$

$$\Psi_1(\mathbf{r}_{23}, \boldsymbol{\rho}_1) \approx \sum\!\!\!\!\!\!\int_n f_n^{(1)}(\boldsymbol{\rho}_1)\varphi_n^{(1)}(\mathbf{r}_{23}), \quad \Psi_2(\mathbf{r}_{13}, \boldsymbol{\rho}_2) \approx \sum\!\!\!\!\!\!\int_{n'} f_{n'}^{(2)}(\boldsymbol{\rho}_2)\varphi_{n'}^{(2)}(\mathbf{r}_{13}).$$

$$\Big[E - H_0 - V_{23}(\vec{r}_{23})\Big]\Psi_1(\vec{r}_{23}, \vec{\rho}_1) = V_{23}(\vec{r}_{23}) \cdot \Big(\Psi_3(\vec{r}_{21}, \vec{\rho}_3) + \Psi_2(\vec{r}_{13}, \vec{\rho}_2)\Big),$$

$$\Big[E - H_0 - V_{13}(\vec{r}_{13})\Big]\Psi_2(\vec{r}_{13}, \vec{\rho}_2) = V_{13}(\vec{r}_{13}) \cdot \Big(\Psi_1(\vec{r}_{23}, \vec{\rho}_1) + \Psi_3(\vec{r}_{21}, \vec{\rho}_3)\Big),$$

$$\Big[E - H_0 - V_{21}(\vec{r}_{21})\Big]\Psi_3(\vec{r}_{21}, \vec{\rho}_3) = V_{21}(\vec{r}_{21}) \cdot \Big(\Psi_2(\vec{r}_{13}, \vec{\rho}_2) + \Psi_1(\vec{r}_{23}, \vec{\rho}_1)\Big).$$

Usual Three-Body Systems

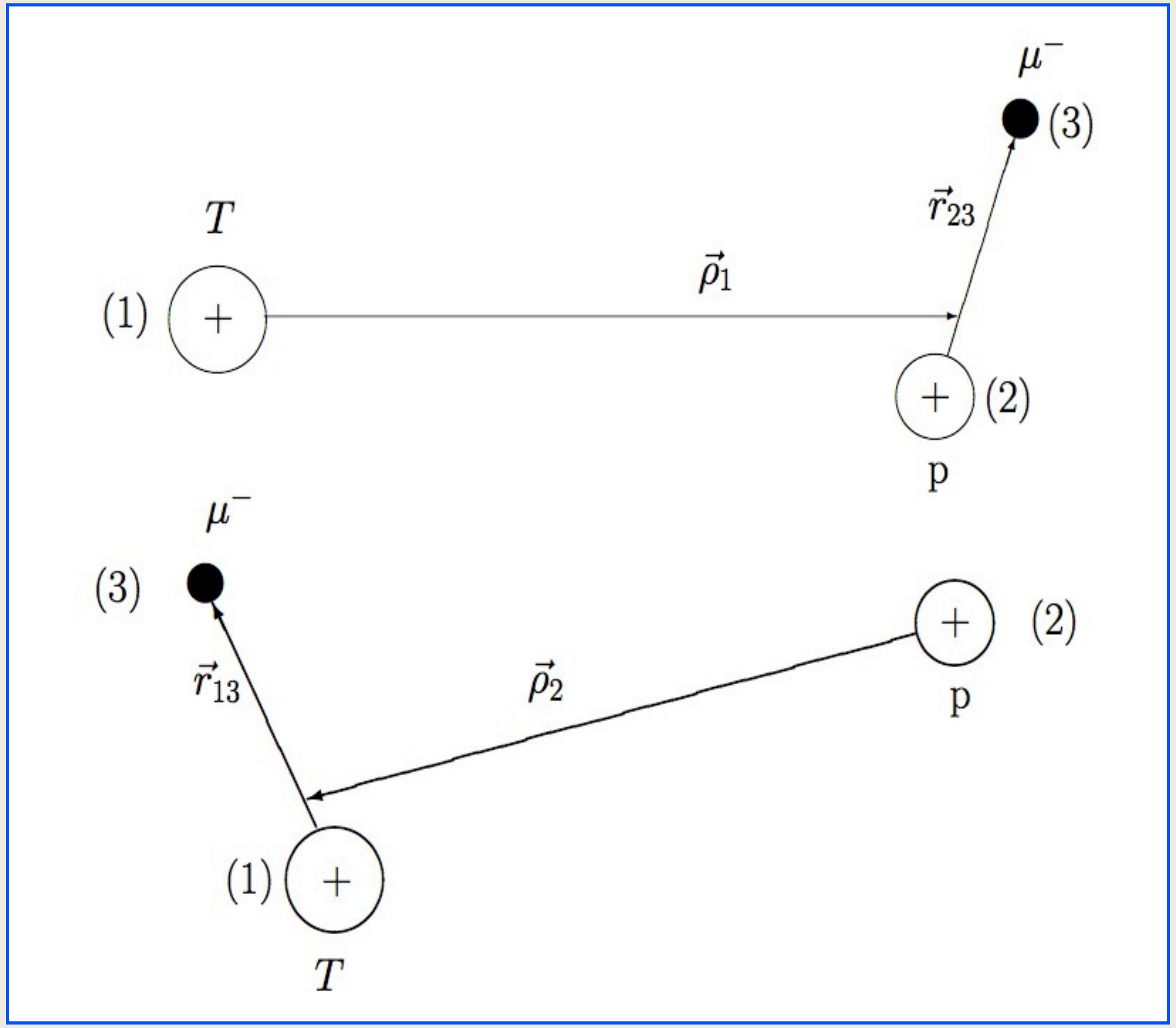

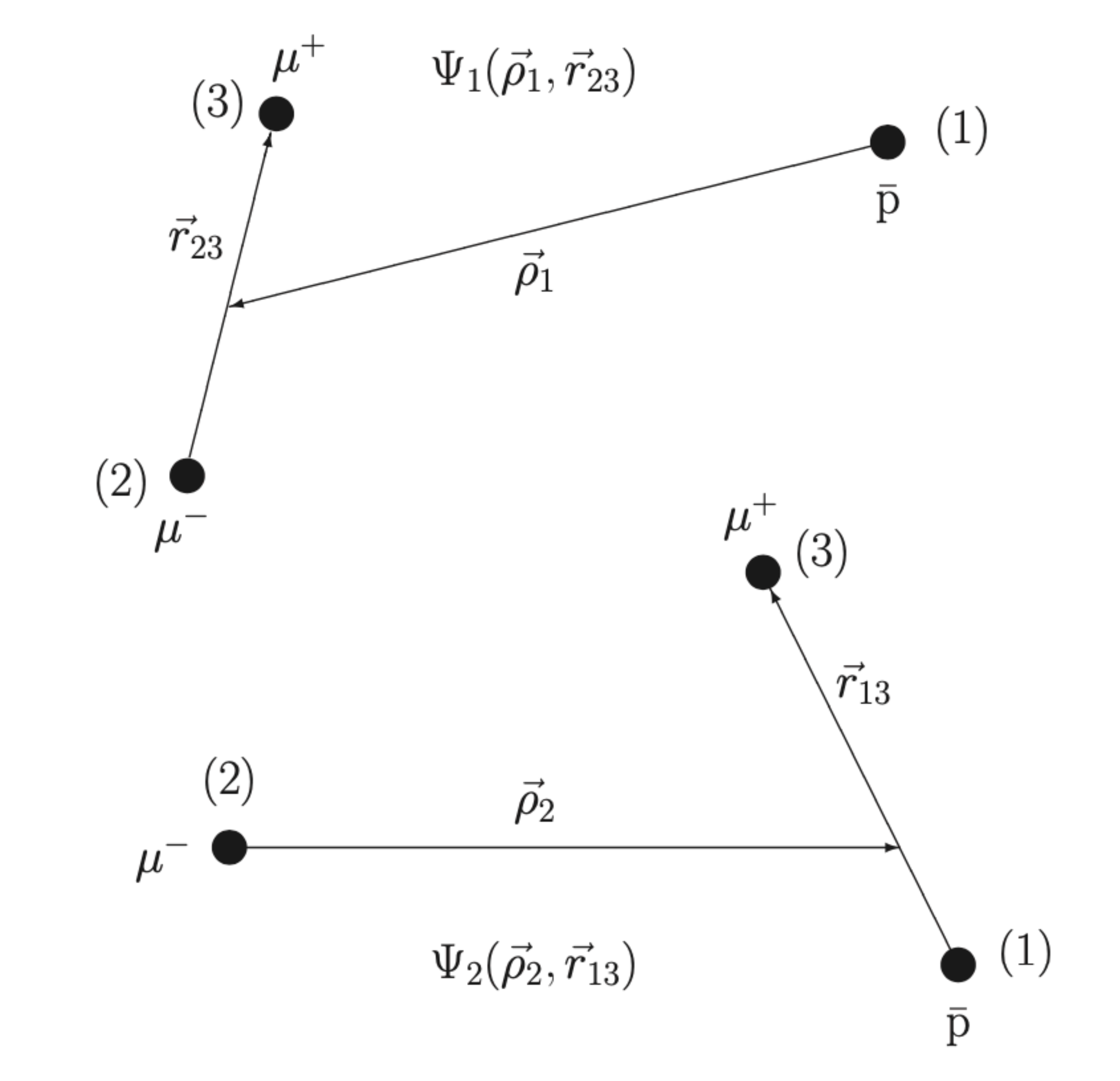
$\Psi_1(\vec{\rho}_1, \vec{r}_{23})$
μ^+
(3)
(1)
$\bar{p}$
$\vec{r}_{23}$
$\vec{\rho}_1$
(2)
μ^-
μ^+
(3)
$\vec{r}_{13}$
(2)
$\vec{\rho}_2$
μ^-
(1)
$\bar{p}$
$\Psi_2(\vec{\rho}_2, \vec{r}_{13})$

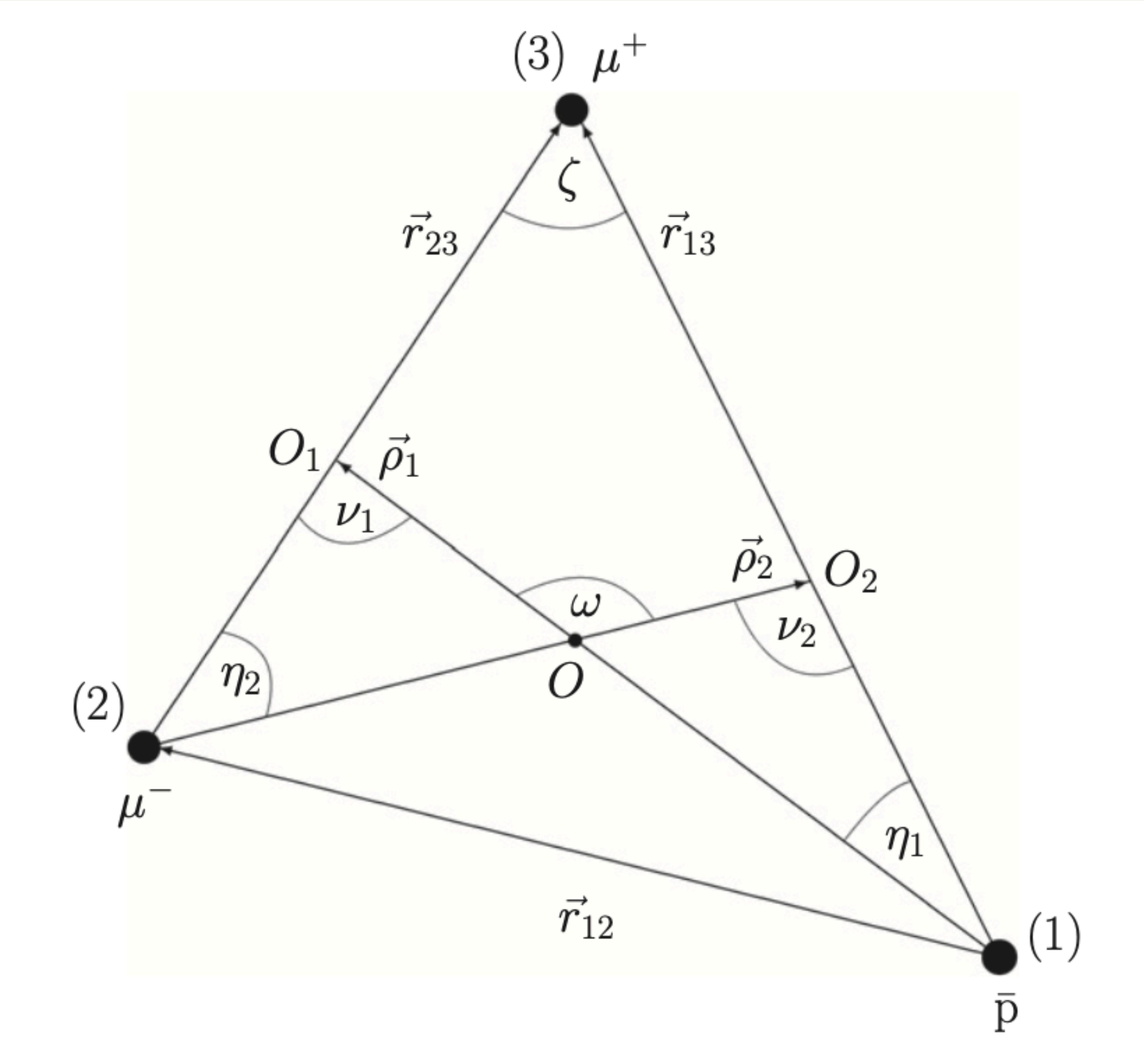
(3) μ^+
ζ
$\vec{r}_{23}$
$\vec{r}_{13}$
O_1
$\vec{\rho}_1$
ν_1
$\vec{\rho}_2$
O_2
ω
ν_2
η_2
O
(2)
μ^-
η_1
$\vec{r}_{12}$
(1)
$\bar{p}$

Unusual Three-Body System

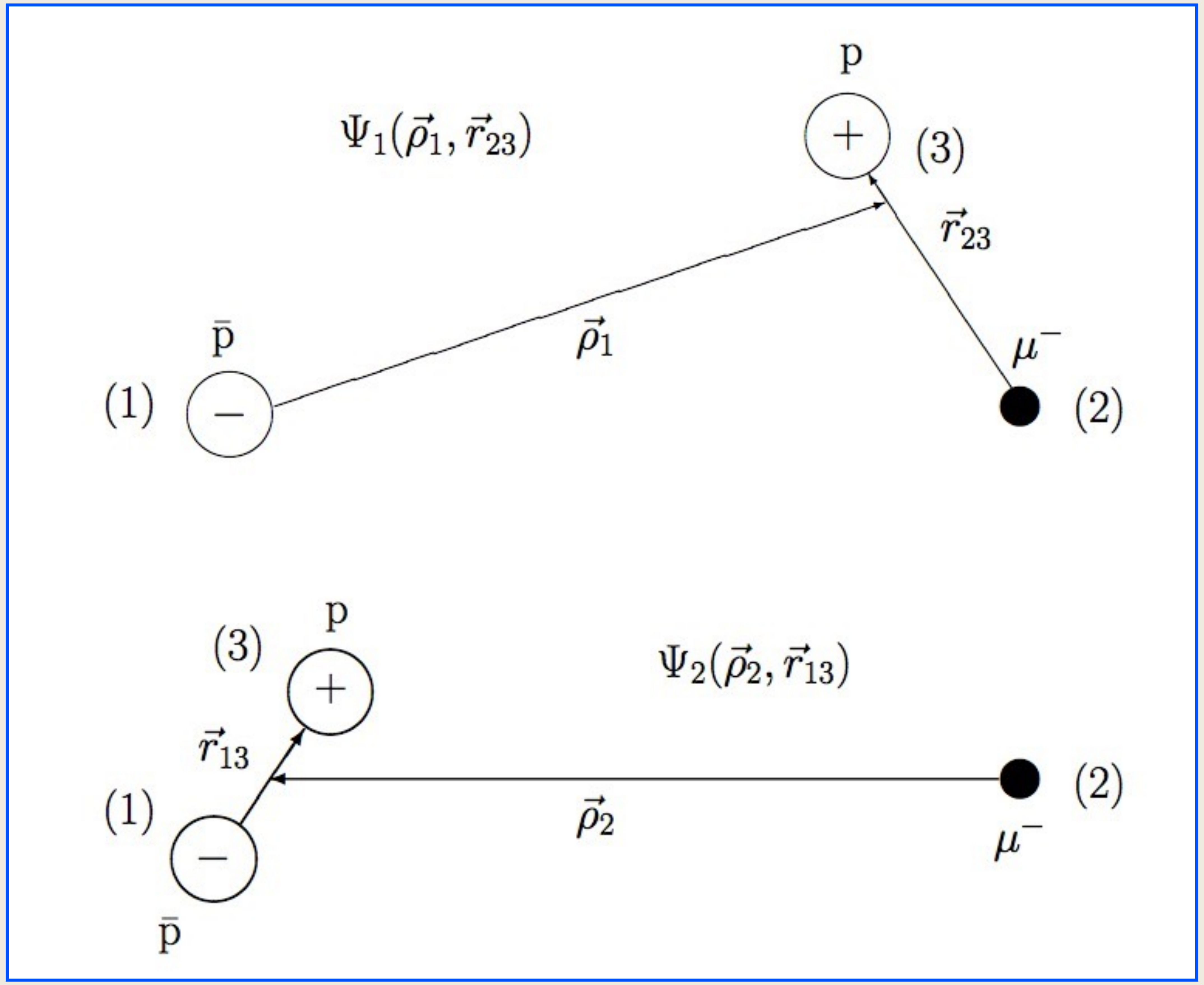

Low-Energy Antiproton Physics(I)

- ***PROBLEMS & fb-systems:***
- Anti-hydrogen (Hbar or $\bar{\mathrm{H}}$) formation reactions.
- Hbar interactions and collisions with hydrogen H, Helium He^{++}, Lithium Li^{+++} etc.
- Slow pbar capture by light atoms He, Li, Be …

- **CERN Experiments: ATRAP, ASACUSA, Gbar etc…**
- Protonium (pbar-p) atom - antiprotonic hydrogen;
- $\bar{\mathrm{p}} - \mathrm{D}$ and $\bar{\mathrm{p}} - \mathrm{T}$ interactions and atomic-type bound systems.
- Strong (nuclear) $\bar{\mathrm{N}}$ - N interaction.

Low-Energy Antiproton Physics(II)

- Positronium: $\mathrm{Ps} = (\mathrm{e}^{+}\mathrm{e}^{-}) + \bar{\mathrm{p}}$,
- True muonium: $(\mu^{+}\mu^{-}) + \bar{\mathrm{p}}$,
- Muonium: $\mathrm{Mu} = (\mu^{+}\mathrm{e}^{-}) + \bar{\mathrm{p}}$,
- Antiparticles: pbar, Hbar,
- Muonic antihydrogen: $\bar{\mathrm{H}}_{\mu} = (\bar{\mathrm{p}}\mu^{+})$,
- Protonium: $\mathrm{Pn} = (\bar{\mathrm{p}}\mathrm{p})$

- *Atomcule:* p^3He^+ & p^4He^+
- $\bar{\mathrm{H}} + \mathrm{H} \to \mathrm{Ps} + \mathrm{Pn}$, $\varepsilon \leqslant 1\mathrm{eV}$,
- $\bar{\mathrm{p}} + \mathrm{Mu} \to \mathrm{H}_{\mu} + \mathrm{e}^{-}$, $\varepsilon \sim$ 1-50 eV,
- Nuclear Few-Body Systems:
- 3-body: $\bar{\mathrm{p}}+\mathrm{D}$,
- 4-body: $\bar{\mathrm{p}}+\mathrm{T}$.

Muon Catalyzed Fusion-μCF cycle

- Coulomb and Coulomb-nuclear few-body systems:
- $(t\mu) + D_2 \rightarrow [(dt\mu)_{L=1} de^-] + e^-$
- $(dt\mu^-)_{L=0} \rightarrow {}^4He^{++} + n + \mu^-$ + 17.6 MeV
- $(dd\mu^-)_{L=1} \rightarrow {}^3He^{++} + n$ + 3.5 MeV

- $(d\mu) + t \rightarrow (t\mu) + d$
- $(p\mu) + t \rightarrow (t\mu) + p$
- $(p\mu) + d \rightarrow (d\mu) + p$
- $(t\mu) + d \rightarrow d + (t\mu)$
- $({}^4He\mu)^+ + p \rightarrow p + \mu^- + {}^4He^{++}$

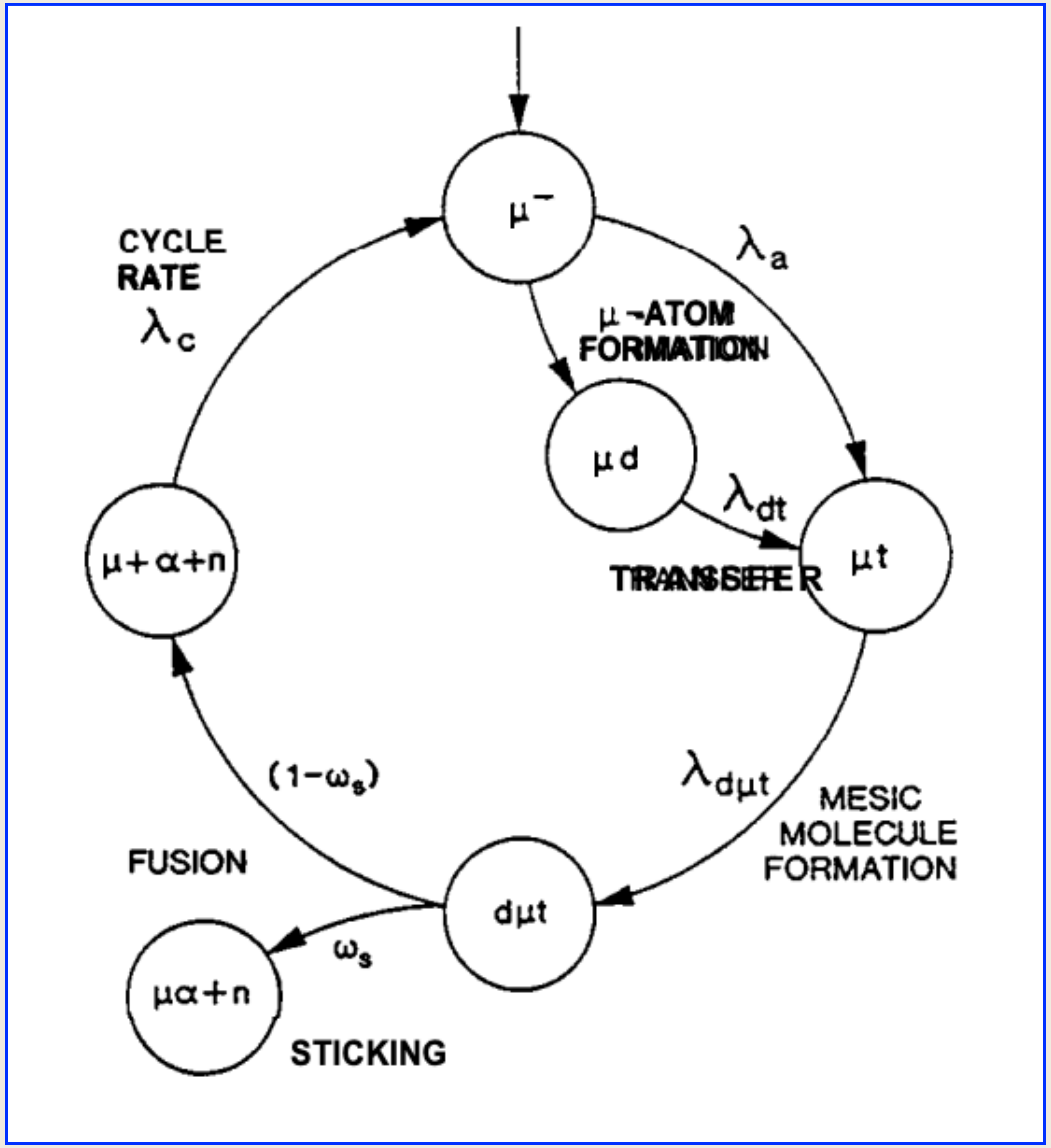
μ⁻
λa
CYCLE
RATE
λc
μ-ATOM
FORMATION
μd
λdt
μt
TRANSFER
μ+α+n
(1−ωs)
λdμt
MESIC
MOLECULE
FORMATION
FUSION
dμt
ωs
μα+n
STICKING

Recent μCF papers

- "Comprehensive Study of muon-catalyzed nuclear reaction processes in the $dt\mu$ molecule", by M. Kamimura et al., Phys. Rev. C **107**, 034607 (2023).
- "Meson-catalyzed fusion in ultra-dense plasmas", by C. Deutsch et al., Phys. Rev. E **98**, 053204 (2018).
- "Experimental determination of the energy dependence of the rate of the muon transfer reaction from muonic hydrogen to oxygen for collision energies up to 0.1 eV", by M. Stoilov et al., Phys. Rev. A **107**, 032823 (2023).
- "Laser-assisted in-flight muon-catalyzed deuteron-triton fusion", by S. Liu et al., Phys. Rev. C **106**, 064611 (2022).
- "Muon Catalyzed Fusion, Present and Future", by Atsuo Iiyoshi et al., AIP Conference Proceedings **2179**, 020010 (2019).
- "Roles of resonant muonic molecule in new kinetics model and muon catalyzed fusion in compressed gas", by T. Yamashita et al., *Sci Rep* **12**, 6393 (2022).

Three-Body Reactions With $\bar{\mathrm{p}}$ and Muons

- **In this work also:**
- Reaction (1):
  $\bar{\mathrm{p}} + (\mathrm{D}\mu^-) \to \bar{\mathrm{p}}\mathrm{D} + \mu^-$,
- Reaction (2):
  $\bar{\mathrm{p}} + (\mathrm{T}\mu^-) \to \bar{\mathrm{p}}\mathrm{T} + \mu^-$,
- Pure Coulomb & Coulomb-nuclear 3-body systems with all heavy particles.

- **Main idea: these reactions can help us to study the strong $\bar{\mathrm{p}}-\mathrm{D}$ and $\bar{\mathrm{p}}-\mathrm{T}$ interactions,**
- This is because the cross sections of the reactions (1) and (2) strongly depend on the nuclear interaction,
- Coulomb is a singular long-range potential.

Basic Equations and Method

- A detailed few-body approach based on three-body Faddeev-type equations is applied.
- These approach is based on decomposition the total three-body wave function into two components.
- A modified close-coupling approach is used.
- It brings an infinite set of coupled integral - differential equations,
- Appropriate rearrangement scattering boundary conditions are applied.

$$\mathbf{r}_{j3} = \mathbf{r}_3 - \mathbf{r}_j,$$
$$\boldsymbol{\rho}_k = (m_3\mathbf{r}_3 + m_j\mathbf{r}_j)/(m_3 + m_j) - \mathbf{r}_k, \quad (j \neq k = 1, 2).$$

$$|\Psi\rangle = \Psi_1(\mathbf{r}_{23}, \boldsymbol{\rho}_1) + \Psi_2(\mathbf{r}_{13}, \boldsymbol{\rho}_2),$$

$$(E - \hat{H}_0 - V_{23}(\mathbf{r}_{23}))\Psi_1(\mathbf{r}_{23}, \boldsymbol{\rho}_1) = (V_{23}(\mathbf{r}_{23}) + V_{12}(\mathbf{r}_{12}))\Psi_2(\mathbf{r}_{13}, \boldsymbol{\rho}_2),$$
$$(E - \hat{H}_0 - V_{13}(\mathbf{r}_{13}))\Psi_2(\mathbf{r}_{13}, \boldsymbol{\rho}_2) = (V_{13}(\mathbf{r}_{13}) + V_{12}(\mathbf{r}_{12}))\Psi_1(\mathbf{r}_{23}, \boldsymbol{\rho}_1).$$

Basic FH-type Equations

1) The constructed coupled equations **satisfy the Schrödinger equation exactly.**

2) The Faddeev decomposition **avoids the over-completeness problems**.

3) Two-body subsystems are treated in an equivalent way.

4) The correct asymptotes are guaranteed.

5) It simplifies the solution procedure and provides the correct asymptotic behavior of the solution below the 3-body break-up threshold.

6) FH-type equations have the same advantages as the Faddeev equations, because they are formulated for the wave function components **with correct physical asymptotes.**

$$\left(E + \frac{1}{2M_k}\Delta_{\boldsymbol{\rho}_k} + \frac{1}{2\mu_j}\Delta_{\mathbf{r}_{j3}} - V_{j3}\right)\Psi_i(\mathbf{r}_{j3}, \boldsymbol{\rho}_k) = \left(V_{j3} + V_{jk}\right)\Psi_{i'}(\mathbf{r}_{k3}, \boldsymbol{\rho}_j),$$

$i \neq i' = 1, 2$, $M_j^{-1} = m_j^{-1} + (m_3 + m_k)^{-1}$, and $\mu_j^{-1} = m_3^{-1} + m_k^{-1}$, where $j \neq k = 1, 2$.

$$\{Y_\lambda(\hat{\rho}) \otimes Y_l(\hat{r})\}_{LM} = \sum_{\mu m} C^{LM}_{\lambda\mu lm} Y_{\lambda\mu}(\hat{\rho}) Y_{lm}(\hat{r}),$$

$$\boxed{\Psi_i(\mathbf{r}_{j3}, \boldsymbol{\rho}_k) = \sum_{LM\lambda l} \Phi^i_{LM\lambda l}(\rho_k, r_{j3})\{Y_\lambda(\hat{\rho}_k) \otimes Y_l(\hat{r}_{j3})\}_{LM}}$$

$$\left(E + \frac{1}{2M_k\rho_k^2}\left\{\frac{\partial}{\partial\rho_k}\left(\rho_k^2\frac{\partial}{\partial\rho_k}\right) - \lambda(\lambda+1)\right\} + \frac{1}{2\mu_j r_{j3}^2}\left\{\frac{\partial}{\partial r_{j3}}\left(r_{j3}^2\frac{\partial}{\partial r_{j3}}\right) - l(l+1)\right\} - V_{j3}\right)\Phi^i_{LM\lambda l}(\rho_k, r_{j3})$$
$$= \int d\hat{\rho}_k \int d\hat{r}_{j3} \sum_{\lambda' l'} W^{(ii')LM}_{\lambda l \lambda' l'} \Phi^{i'}_{LM\lambda' l'}(\rho_j, r_{k3}), \tag{12}$$

$$W^{(ii')LM}_{\lambda l \lambda' l'} = \left\{Y_\lambda(\hat{\rho}_k) \otimes Y_l(\hat{r}_{j3})\right\}^*_{LM} \left(V_{j3} + V_{jk}\right) \left\{Y_{\lambda'}(\hat{\rho}_j) \otimes Y_{l'}(\hat{r}_{k3})\right\}_{LM}. \tag{13}$$

To progress from (12) to one-dimensional equations, we apply a modified close coupling method, which consists of expanding each component of the wave function $\Psi_i(\mathbf{r}_{j3}, \boldsymbol{\rho}_k)$ over the Hamiltonian eigenfunctions of subsystems:

$$\hat{h}_{j3} = -\frac{1}{2\mu_j}\nabla^2_{\mathbf{r}_{j3}} + V_{j3}(\mathbf{r}_{j3}). \tag{14}$$

Thus, following expansions can be applied:

$$\Phi^i_{LM\lambda l}(\rho_k, r_{j3}) = \frac{1}{\rho_k}\sum_n f^{(i)LM}_{nl\lambda}(\rho_k) R^{(i)}_{nl}(r_{j3}), \tag{15}$$

where functions $R^{(i)}_{nl}(r_{j3})$ are defined by the following equation:

$$\left(E^i_n + \frac{1}{2\mu_j r^2_{j3}}\left\{\frac{\partial}{\partial r_{j3}}\left(r^2_{j3}\frac{\partial}{\partial r_{j3}}\right) - l(l+1)\right\} - V_{j3}\right) R^{(i)}_{nl}(r_{j3}) = 0. \tag{16}$$

Substituting Eq. (15) into (12), multiplying by the corresponding functions $R_{nl}^{(i)}(r_{j3})$ and integrating over $r_{j3}^2 dr_{j3}$ yields a set of integral–differential equations for the unknown functions $f_{nl\lambda}^{(i)}(\rho_k)$:

$$2M_k(E - E_n^i) f_\alpha^{(i)}(\rho_k) + \left(\frac{\partial^2}{\partial \rho_k^2} - \frac{\lambda(\lambda+1)}{\rho_k^2}\right) f_\alpha^{(i)}(\rho_k)$$

$$= 2M_k \sum_\alpha \int_0^\infty dr_{j3} r_{j3}^2 \int d\hat{r}_{j3} \int d\hat{\rho}_k \frac{\rho_k}{\rho_j} Q_{\alpha\alpha'}^{ii'} f_{\alpha'}^{(i')}(\rho_j), \quad (17)$$

where

$$Q_{\alpha\alpha'}^{ii'} = R_{nl}^{(i)}(r_{j3}) W_{\lambda l \lambda' l'}^{(ii')LM} R_{n'l'}^{(i')}(r_{k3}). \quad (18)$$

For brevity one can denote $\alpha \equiv nl\lambda$ ($\alpha' \equiv n'l'\lambda'$), and omit LM because all functions have to be the same. The functions $f_\alpha^{(i)}(\rho_k)$ depend on the scalar argument, but this set is still not one-dimensional, because formulas are used in different frames of the Jacobi coordinates:

$$\boldsymbol{\rho}_j = \mathbf{r}_{j3} - \beta_k \mathbf{r}_{k3}, \tag{19}$$

$$\mathbf{r}_{j3} = \frac{1}{\gamma}(\beta_k \boldsymbol{\rho}_k + \boldsymbol{\rho}_j), \tag{20}$$

$$\mathbf{r}_{jk} = \frac{1}{\gamma}(\sigma_j \boldsymbol{\rho}_j - \sigma_k \boldsymbol{\rho}_k), \tag{21}$$

with the following mass coefficients:

$$\beta_k = m_k/(m_3 + m_k), \quad \sigma_k = 1 - \beta_k, \tag{22}$$

$$\gamma = 1 - \beta_k \beta_j, \quad (j \neq k = 1, 2), \tag{23}$$

which clearly demonstrates that the modulus of $\boldsymbol{\rho}_j$ depends on two vectors, over which integration on the right-hand sides is accomplished. It follows from Eq. (20), that: $\boldsymbol{\rho}_j = \gamma \mathbf{r}_{j3} - \beta_k \boldsymbol{\rho}_k$. Therefore, to obtain one-dimensional integral–differential equations, corresponding to Eq. (17), we will proceed with the integration over variables $\{\boldsymbol{\rho}_j, \hat{\rho}_k\}$, rather than $\{\mathbf{r}_{j3}, \hat{\rho}_k\}$. The Jacobian of this transformation is $J = \gamma^{-3}$. Thus, we arrive at a set of one-dimensional integral–differential equations:

$$2M_k(E - E_n^i) f_\alpha^{(i)}(\rho_k) + \left(\frac{\partial^2}{\partial \rho_k^2} - \frac{\lambda(\lambda+1)}{\rho_k^2}\right) f_\alpha^{(i)}(\rho_k) = \frac{M_k}{\gamma^{-3}} \sum_{\alpha'} \int_0^\infty d\rho_j S_{\alpha\alpha'}^{ii'}(\rho_j, \rho_k) f_{\alpha'}^{(i')}(\rho_j), \tag{24}$$

$$S_{\alpha\alpha'}^{ii'}(\rho_j, \rho_k) = 2\rho_j \rho_k \int d\hat{\rho}_j \int d\hat{\rho}_k R_{nl}^{(i)}(r_{j3}) \left\{Y_\lambda(\hat{\rho}_k) \otimes Y_l(\hat{r}_{j3})\right\}_{LM}^* \left(V_{j3} + V_{jk}\right) \times \left\{Y_{\lambda'}(\hat{\rho}_j) \otimes Y_{l'}(\hat{r}_{k3})\right\}_{LM} R_{n'l'}^{(i')}(r_{k3}). \tag{25}$$

$$S_{\alpha\alpha'}^{ii'}(\rho_j, \rho_k) = \frac{4\pi}{2L+1} [(2\lambda+1)(2\lambda'+1)]^{\frac{1}{2}} \rho_j \rho_k \int_0^\pi d\omega \sin\omega R_{nl}^{(i)}(r_{j3}) \left(V_{j3}(r_{j3}) + V_{jk}(r_{jk})\right) \times R_{n'l'}^{(i')}(r_{k3}) \sum_{mm'} D_{mm'}^L(0, \omega, 0) C_{\lambda 0 l m}^{Lm} C_{\lambda' 0 l' m'}^{Lm'} Y_{lm}(\nu_j, \pi) Y_{l'm'}^*(\nu_k, \pi)\ , \tag{26}$$

Final Set of Coupled Integral-Differential Equations

$$\left[(k_n^i)^2 + \frac{\partial^2}{\partial \rho_i^2} - \frac{\lambda(\lambda+1)}{\rho_i^2}\right] f_\alpha^{(i)}(\rho_i) = g_i \sum_{\alpha'} \sqrt{\frac{(2\lambda+1)(2\lambda'+1)}{(2L+1)^2}} \int_0^\infty d\rho_{i'} f_{\alpha'}^{(i')}(\rho_{i'})$$
$$\times \int_0^\pi d\omega \sin\omega R_{nl}^{(i)}(r_{i'3}) \Big(V_{i'3}(r_{i'3}) + V_{ii'}(r_{ii'})\Big) R_{n'l'}^{(i')}(r_{i3}) \rho_{i'} \rho_i$$
$$\times \sum_{mm'} D_{mm'}^L(0,\omega,0) C_{\lambda 0 lm}^{Lm} C_{\lambda' 0 l'm'}^{Lm'} Y_{lm}(\nu_i,\pi) Y_{l'm'}^*(\nu_{i'},\pi). \tag{27}$$

For the sake of simplicity $\alpha \equiv (nl\lambda)$ are quantum numbers of a three-body state and L is the total angular momentum of the three-body system, $i \neq i' = 1, 2$, $g_i = 4\pi M_i/\gamma^3$, $k_n^i = \sqrt{2M_i(E - E_n^{i'})}$, where $E_n^{i'}$ is the binding energy of the subsystem $(i'3)$, $M_1 = m_1(m_2 + m_3)/(m_1 + m_2 + m_3)$ and $M_2 = m_2(m_1 + m_3)/(m_1+m_2+m_3)$ are the reduced masses, $\gamma = 1 - m_i m_{i'}/((m_i+m_3)(m_{i'}+m_3))$, $D_{mm'}^L(0,\omega,0)$ the Wigner functions, $C_{\lambda 0 lm}^{Lm}$ the Clebsh–Gordon coefficients, Y_{lm} are the spherical functions, ω is the angle between the Jacobi coordinates $\boldsymbol{\rho}_i$ and $\boldsymbol{\rho}_{i'}$, ν_i is the angle between $\mathbf{r}_{i'3}$ and $\boldsymbol{\rho}_i$, $\nu_{i'}$ is the angle between $\mathbf{r}_{i3}$ and $\boldsymbol{\rho}_{i'}$. One can show that: $\sin\nu_i = \rho_{i'}/(\gamma r_{i'3}) \sin\omega$ and $\cos\nu_i = (\beta_i \rho_i + \rho_{i'} \cos\omega)/(\gamma r_{i'3})$.

$$\begin{cases} f_{1s}^{(i)}(\rho_i) \underset{\rho_i \to +\infty}{\sim} \sin(k_{n=1}^{(i)}\rho_i) + K_{ii}\cos(k_{n=1}^{(i)}\rho_i) \\ f_{1s}^{(j)}(\rho_j) \underset{\rho_j \to +\infty}{\sim} \sqrt{v_i/v_j}\,K_{ij}\cos(k_{n=1}^{(j)}\rho_j) \end{cases}$$

$$f_{nl}^{(i)}(0) \sim 0.$$

$$\begin{cases} f_{1s}^{(1)}(\rho_1) \underset{\rho_1 \to +\infty}{\sim} \sin(k_1^{(1)}\rho_1) + K_{11}\cos(k_1^{(1)}\rho_1), \\ f_{1s}^{(2)}(\rho_2) \underset{\rho_2 \to +\infty}{\sim} \sqrt{v_1/v_2}\,K_{12}\cos(k_1^{(2)}\rho_2), \end{cases}$$

$$\begin{cases} f_{1s}^{(1)}(\rho_1) \underset{\rho_1 \to +\infty}{\sim} \sqrt{v_2/v_1}\,K_{21}\cos(k_1^{(1)}\rho_1), \\ f_{1s}^{(2)}(\rho_2) \underset{\rho_2 \to +\infty}{\sim} \sin(k_1^{(2)}\rho_2) + K_{22}\cos(k_1^{(2)}\rho_2), \end{cases}$$

Final Set of Coupled Integral-Differential Equations

$$\left[\left(k_n^{(1)}\right)^2 + \frac{\partial^2}{\partial\rho_1^2} - \frac{\lambda(\lambda+1)}{\rho_1^2}\right] f_\alpha^{(1)}(\rho_1) = g_1 \sum_{\alpha'} \frac{\sqrt{(2\lambda+1)(2\lambda'+1)}}{2L+1} \int_0^\infty \mathrm{d}\rho_2 f_{\alpha'}^{(2)}(\rho_2)$$
$$\times \int_0^\pi \mathrm{d}\omega \sin\omega R_{nl}^{(1)}(|\vec{r}_{23}|)\left[-\frac{1}{|\vec{r}_{23}|} + \frac{Z_1}{|\vec{r}_{12}|}\right] R_{n'l'}^{(2)}(|\vec{r}_{13}|)\rho_1\rho_2$$
$$\times \sum_{mm'} D_{mm'}^L(0,\omega,0) C_{\lambda 0 lm}^{Lm} C_{\lambda' 0 l'm'}^{Lm'} Y_{lm}^*(\nu_1,\pi) Y_{l'm'}(\nu_2,\pi),$$

$$\left[\left(k_n^{(2)}\right)^2 + \frac{\partial^2}{\partial\rho_2^2} - \frac{\lambda'(\lambda'+1)}{\rho_2^2}\right] f_\alpha^{(2)}(\rho_2) = g_2 \sum_{\alpha'} \frac{\sqrt{(2\lambda+1)(2\lambda'+1)}}{2L+1} \int_0^\infty \mathrm{d}\rho_1 f_{\alpha'}^{(1)}(\rho_1)$$
$$\times \int_0^\pi \mathrm{d}\omega \sin\omega R_{nl}^{(2)}(|\vec{r}_{13}|)\left[-\frac{Z_1}{|\vec{r}_{13}|} + \frac{Z_1}{|\vec{r}_{12}|}\right] R_{n'l'}^{(1)}(|\vec{r}_{23}|)\rho_2\rho_1$$
$$\times \sum_{mm'} D_{mm'}^L(0,\omega,0) C_{\lambda 0 lm}^{Lm} C_{\lambda' 0 l'm'}^{Lm'} Y_{lm}^*(\nu_2,\pi) Y_{l'm'}(\nu_1,\pi).$$

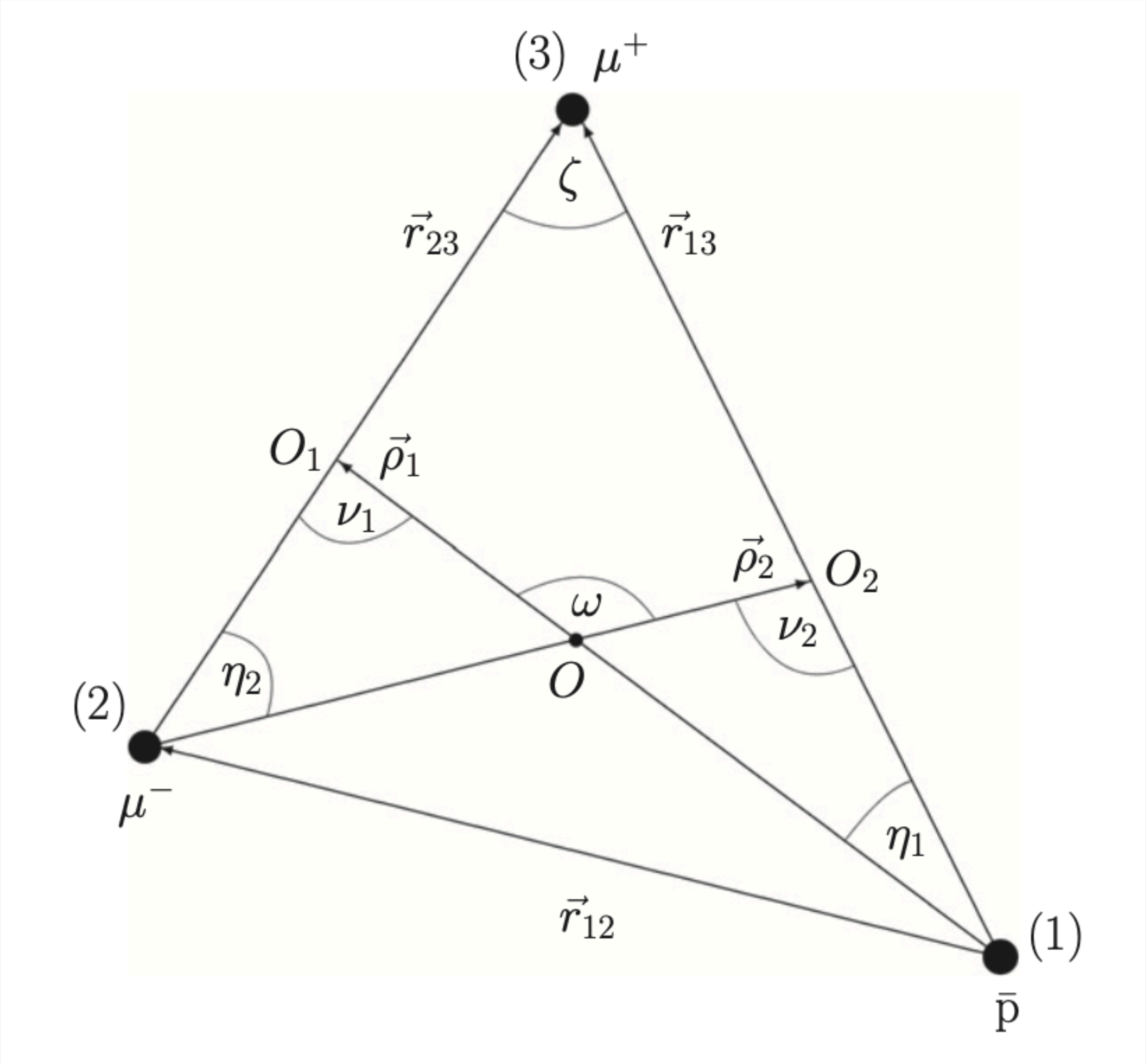
(3) μ^+
ζ
$\vec{r}_{23}$
$\vec{r}_{13}$
O_1
$\vec{\rho}_1$
ν_1
$\vec{\rho}_2$
O_2
ω
ν_2
η_2
O
(2)
μ^-
η_1
$\vec{r}_{12}$
(1)
$\bar{\mathrm{p}}$

Reaction Cross-Sections: K-matrix Approach

$$\mathrm{f}_{1s}^{(i)}(\rho_i) = f_{1s}^{(i)}(\rho_i) - \sin(k_{n=1}^{(i)}\rho_i),$$

$$\sigma_{ij} = \frac{4\pi}{k_{n=1}^{(i)2}} \left| \frac{\mathbf{K}}{1 - \mathbf{iK}} \right|^2 = \frac{4\pi}{k_{n=1}^{(i)2}} \frac{\delta_{ij} D^2 + K_{ij}^2}{(D-1)^2 + (K_{11} + K_{22})^2},$$

$$\mathbf{K} = \begin{pmatrix} K_{11} & K_{12} \\ K_{21} & K_{22} \end{pmatrix}$$

$$\chi(E) = K_{12}/K_{21} = 1.0,$$

$$S^{(ii')}_{\alpha\alpha'}(\rho_i,\rho_{i'}) = \frac{4\pi}{\beta_i}\frac{[(2\lambda+1)(2\lambda'+1)]^{\frac{1}{2}}}{2L+1}\int\limits_{|\beta_i\rho_i-\rho_{i'}|}^{(\beta_i\rho_i+\rho_{i'})} dx\, R^{(i)}_{nl}(x)\left[-1+\frac{x}{r_{ii'}(x)}\right] R^{(i')}_{n'l'}(r_{i3}(x))$$

$$\times \sum_{mm'} D^{L}_{mm'}(0,\omega(x),0)\, C^{Lm}_{\lambda 0 lm}\, C^{Lm'}_{\lambda' 0 l'm'}\, Y_{lm}(\nu_i(x),\pi)\, Y^{*}_{l'm'}(\nu_{i'}(x),\pi).$$

Discretization Procedure

$$\left[k_n^{(1)2} + D_{ij}^2 - \frac{\lambda(\lambda+1)}{\rho_{1i}^2}\right] f_\alpha^{(1)}(i) - \frac{M_1}{\gamma^3} \sum_{\alpha'=1}^{N_s} \sum_{j=1}^{N_p} w_j S_{\alpha\alpha'}^{(12)}(\rho_{1i}, \rho_{2j}) f_{\alpha'}^{(2)}(j) = 0,$$

$$-\frac{M_2}{\gamma^3} \sum_{\alpha=1}^{N_s} \sum_{j=1}^{N_p} w_j S_{\alpha'\alpha}^{(21)}(\rho_{2i}, \rho_{1j}) f_\alpha^{(1)}(j) + \left[k_{n'}^{(2)2} + D_{ij}^2 - \frac{\lambda'(\lambda'+1)}{\rho_{2i}^2}\right] f_{\alpha'}^{(2)}(i) = B_{\alpha'}^{21}(i).$$

$$D_{ij}^2 f_\alpha(i) = (f_\alpha(i-1)\delta_{i-1,j} - 2f_\alpha(i)\delta_{i,j} + f_\alpha(i+1)\delta_{i+1,j})/\Delta,$$

$$B_{\alpha'}^{(21)}(i) = M_2/\gamma^3 \sum_{j=1}^{N_p} w_j S_{\alpha' 1s0}^{(21)}(i,j) \sin(k_1 \rho_j),$$

	1s′	2s′	2p′				
1s		**A**=0…	0…	$-\frac{M_1}{\gamma^3} S^{(12)}_{1s:1s'}$	$-\frac{M_1}{\gamma^3} S^{(12)}_{1s:2s'}$	$-\frac{M_1}{\gamma^3} S^{(12)}_{1s:2p'}$	
2s	0…		0…	$-\frac{M_1}{\gamma^3} S^{(12)}_{2s:1s'}$	$-\frac{M_1}{\gamma^3} S^{(12)}_{2s:2s'}$	$-\frac{M_1}{\gamma^3} S^{(12)}_{2s:2p'}$	
2p	0…	0…		$-\frac{M_1}{\gamma^3} S^{(12)}_{2p:1s'}$	$-\frac{M_1}{\gamma^3} S^{(12)}_{2p:2s'}$	$-\frac{M_1}{\gamma^3} S^{(12)}_{2p:2p'}$	
	$-\frac{M_2}{\gamma^3} S^{(21)}_{1s':1s}$	$-\frac{M_2}{\gamma^3} S^{(21)}_{1s':2s}$	$-\frac{M_2}{\gamma^3} S^{(21)}_{1s':2p}$		**A**=0…	0…	1s′
	$-\frac{M_2}{\gamma^3} S^{(21)}_{2s':1s}$	$-\frac{M_2}{\gamma^3} S^{(21)}_{2s':2s}$	$-\frac{M_2}{\gamma^3} S^{(21)}_{2s':2p}$	0…		0…	2s′
	$-\frac{M_2}{\gamma^3} S^{(21)}_{2p':1s}$	$-\frac{M_2}{\gamma^3} S^{(21)}_{2p':2s}$	$-\frac{M_2}{\gamma^3} S^{(21)}_{2p':2p}$	0…	0…		2p′
				1s	2s	2p	

$$\sum_{\alpha'=1}^{2\times N_s} \sum_{j=1}^{N_p} \mathbf{A}_{\alpha\alpha'}(i,j)\vec{f}_{\alpha'}(j) = \vec{b}_{\alpha}(i).$$

$$S^{(ii')}_{\alpha\alpha'}(\rho_i,\rho_{i'}) = \frac{4\pi}{\beta_i}\frac{[(2\lambda+1)(2\lambda'+1)]^{\frac{1}{2}}}{2L+1}\int_{|\beta_i\rho_i-\rho_{i'}|}^{\beta_i\rho_i+\rho_{i'}} dx R^{(i)}_{nl}(x)\left[-1+\frac{x}{r_{ii'}(x)}\right]R^{(i')}_{n'l'}(r_{i3}(x))$$
$$\sum_{mm'} D^{L}_{mm'}(0,\omega(x),0)C^{Lm}_{\lambda 0lm}C^{Lm'}_{\lambda'0l'm'}Y_{lm}(\nu_i(x),\pi)Y^{*}_{l'm'}(\nu_{i'}(x),\pi). \quad (40)$$

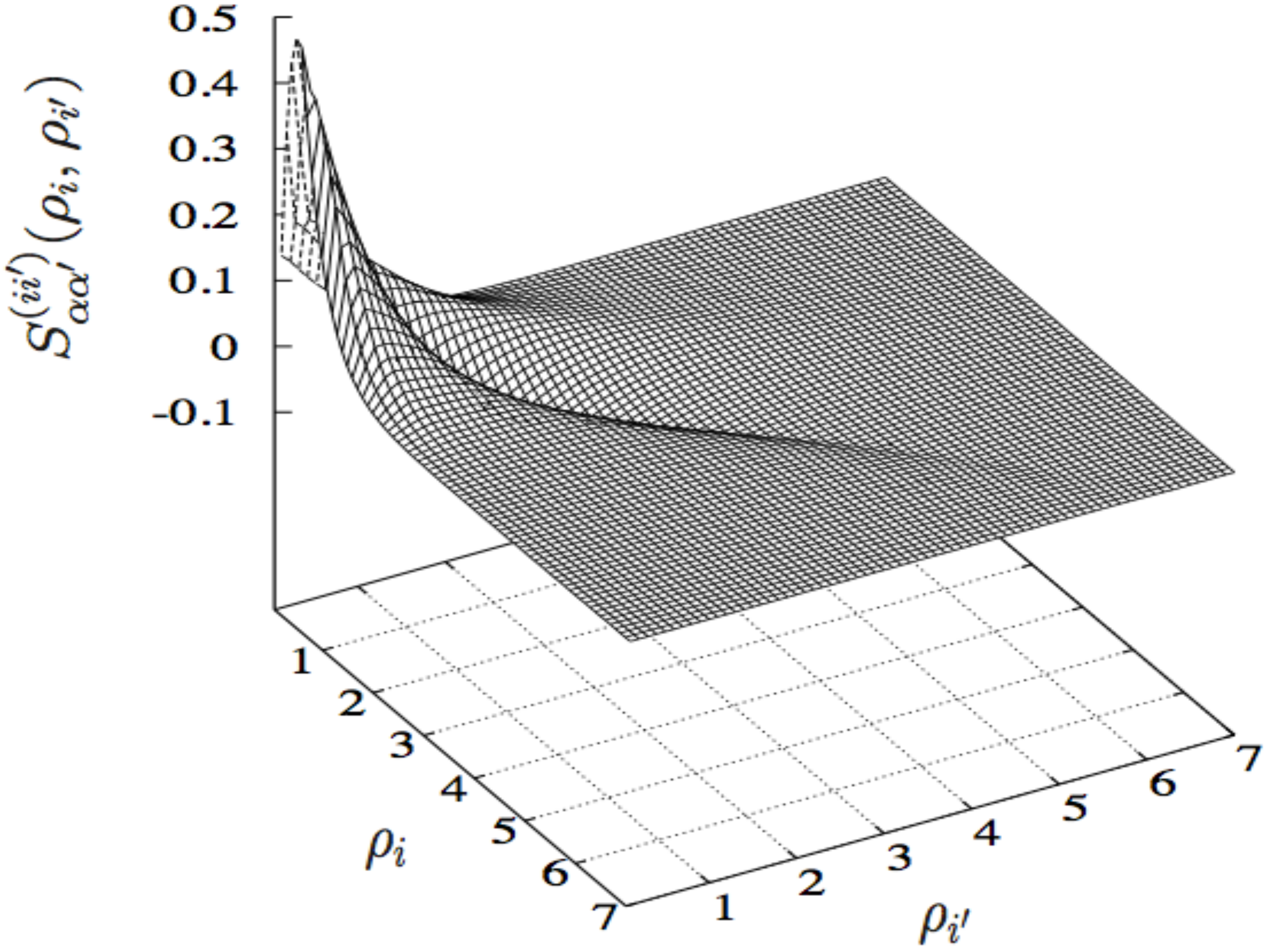

FIG. 3. The angular integral $S^{ii'}_{\alpha\alpha'}(\rho_i, \rho_{i'})$, Eq. (40), in the input channel $\overline{\mathrm{p}} + (\mu^+\mu^-)$ when α =1s and α' =1s.

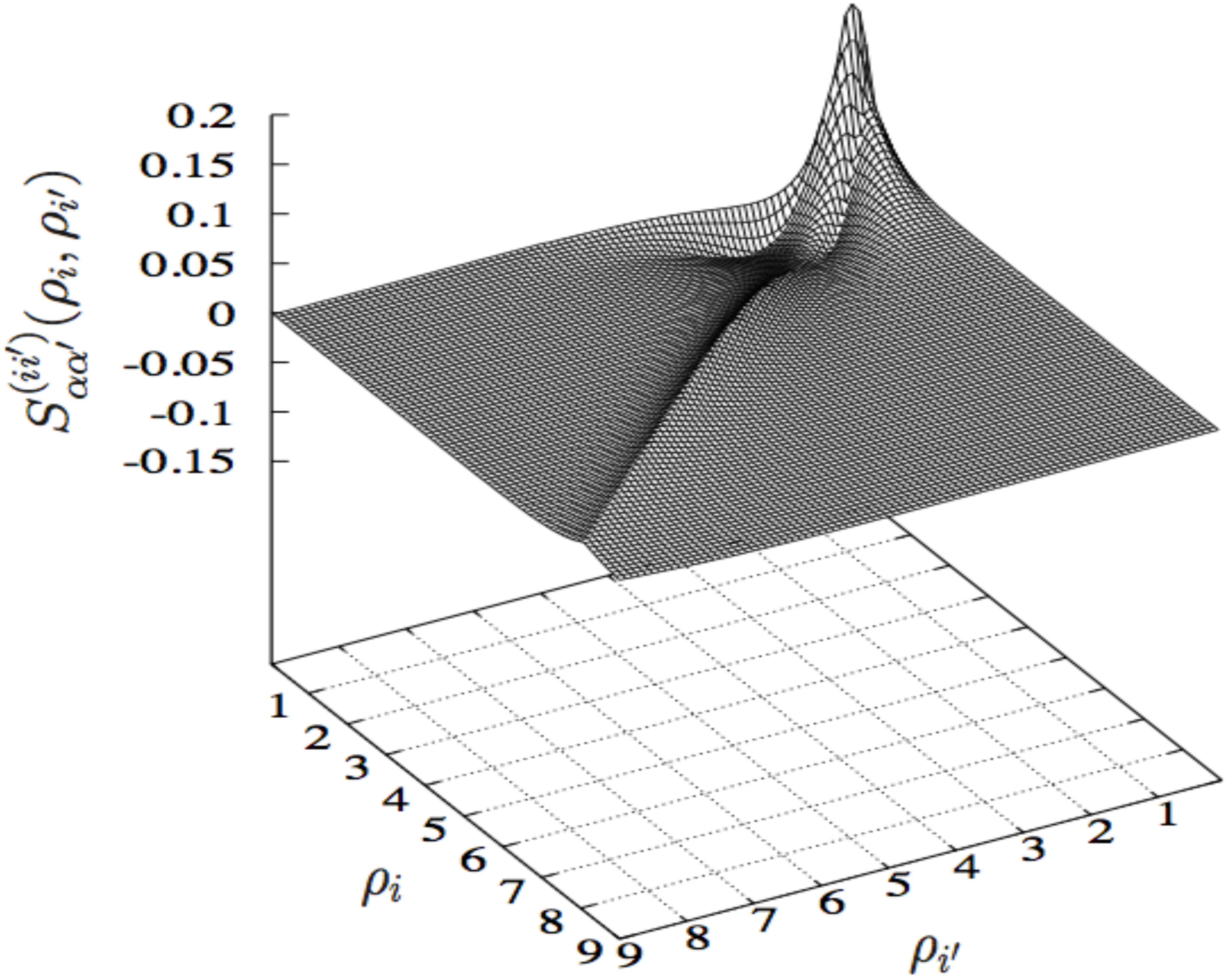

FIG. 4. The angular integral $S^{ii'}_{\alpha\alpha'}(\rho_i, \rho_{i'})$, Eq. (40), in the input channel $\overline{\mathrm{p}} + (\mu^+\mu^-)$ when $\alpha =$1s and $\alpha' =$2s.

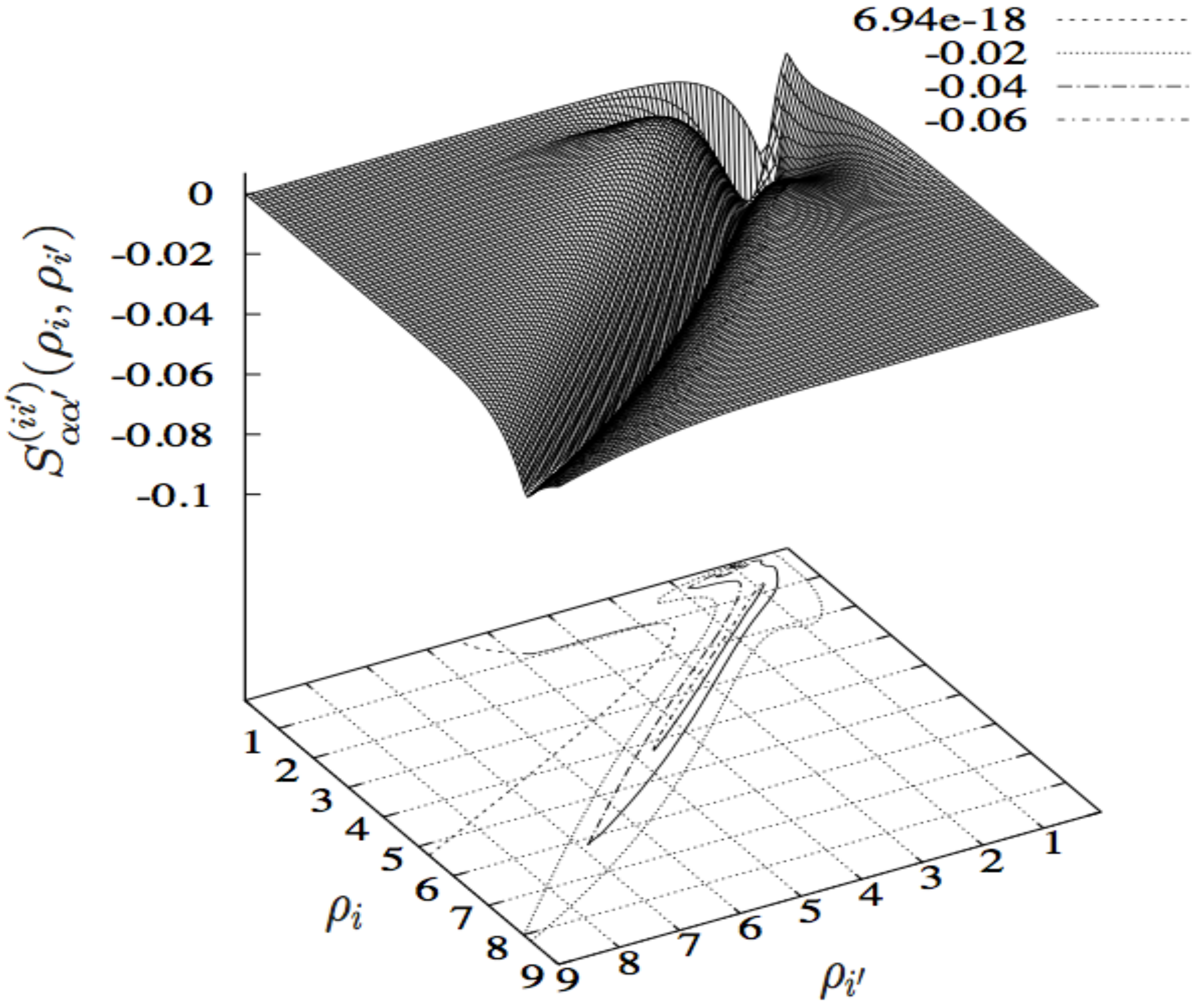

FIG. 5. The angular integral $S^{ii'}_{\alpha\alpha'}(\rho_i, \rho_{i'})$, Eq. (40), in the input channel $\overline{\mathrm{p}} + (\mu^+\mu^-)$ when α =1s and α' =2p.

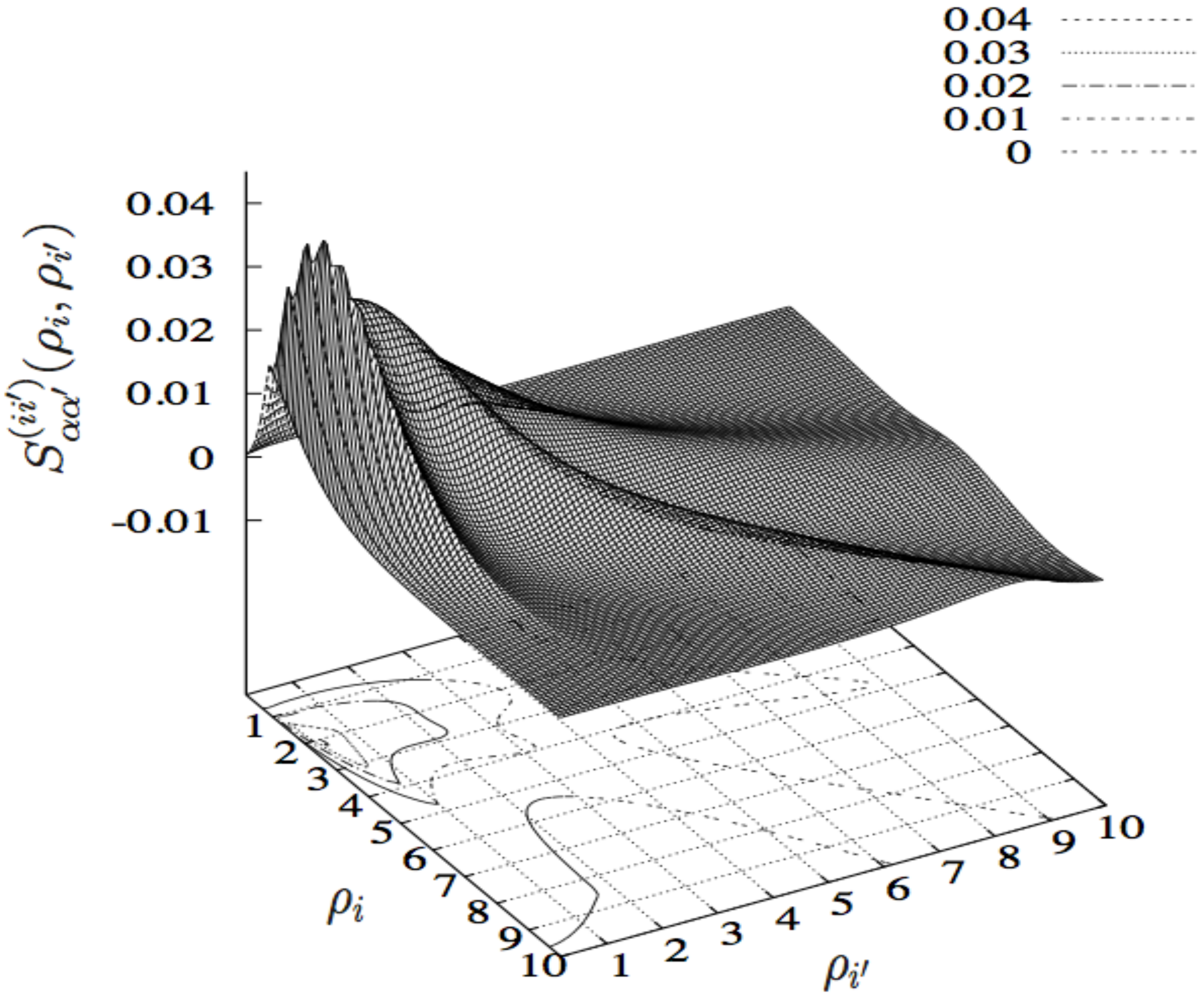

FIG. 6. The angular integral $S^{ii'}_{\alpha\alpha'}(\rho_i,\rho_{i'})$, Eq. (40), in the input channel $\overline{\mathrm{p}}+(\mu^+\mu^-)$ when α =2p and α' =2p.

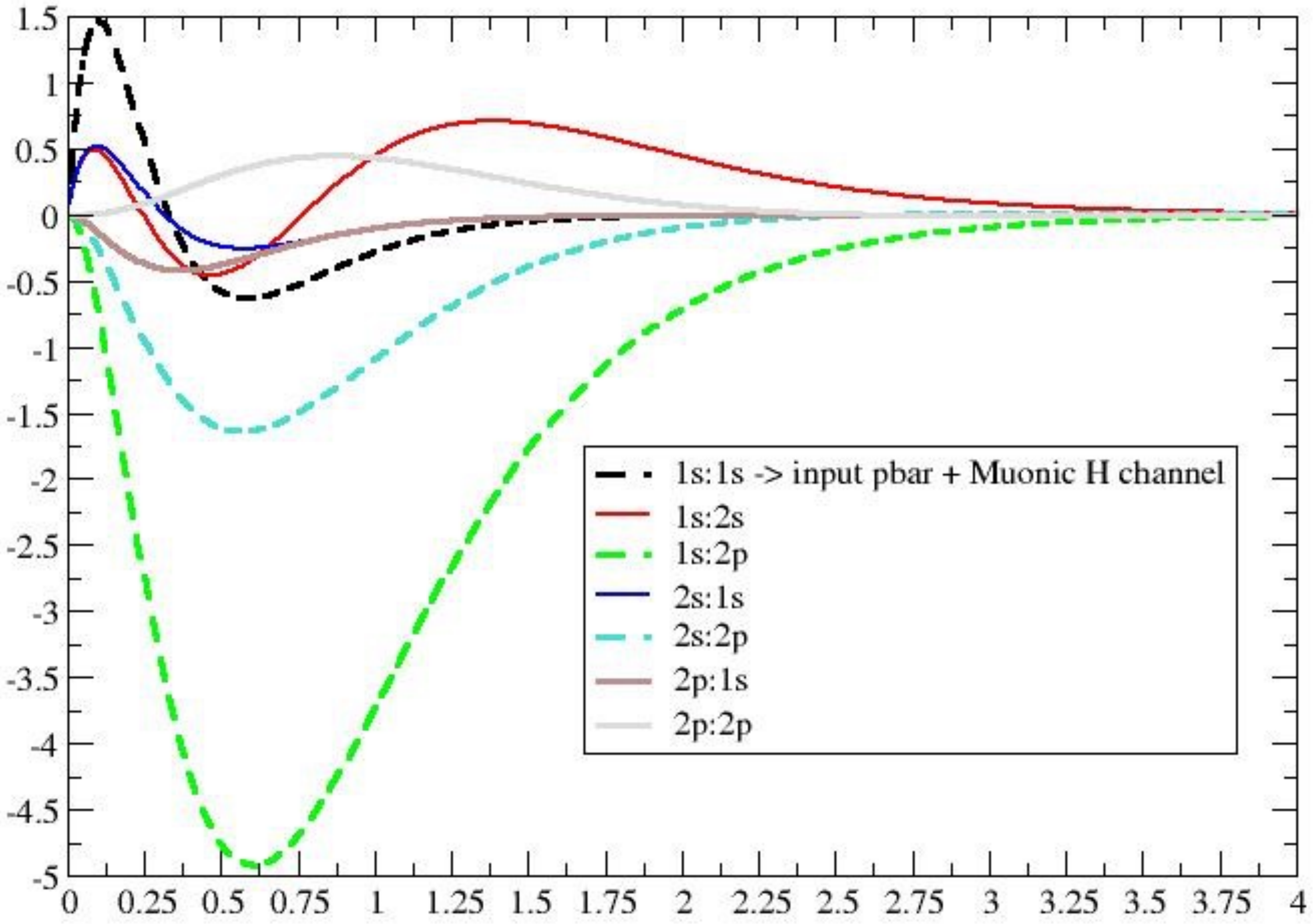
1s:1s -> input pbar + Muonic H channel
1s:2s
1s:2p
2s:1s
2s:2p
2p:1s
2p:2p
1.5
1
0.5
0
-0.5
-1
-1.5
-2
-2.5
-3
-3.5
-4
-4.5
-5
0
0.25
0.5
0.75
1
1.25
1.5
1.75
2
2.25
2.5
2.75
3
3.25
3.5
3.75
4

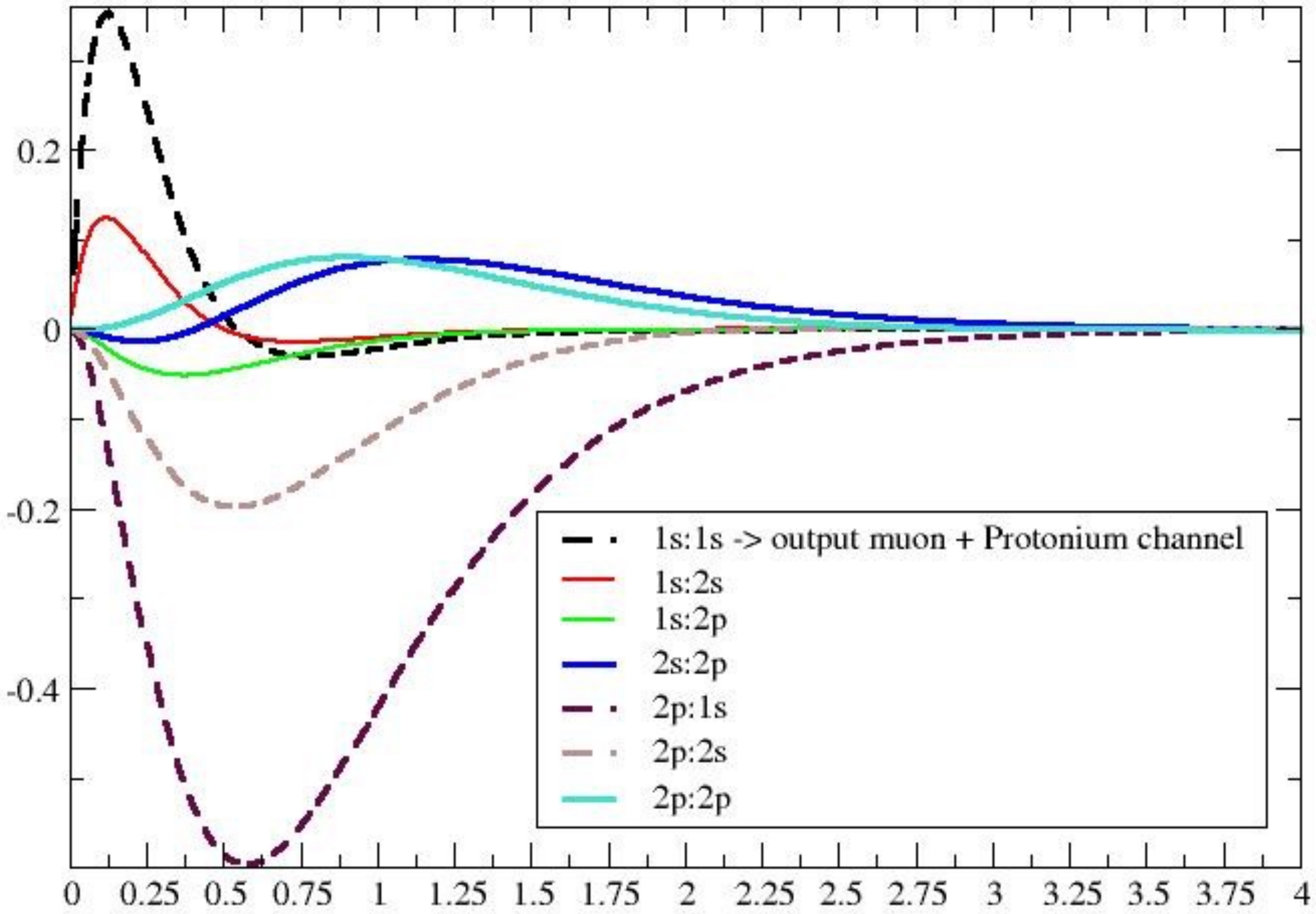

0.2
0
-0.2
-0.4
0
0.25
0.5
0.75
1
1.25
1.5
1.75
2
2.25
2.5
2.75
3
3.25
3.5
3.75
4
1s:1s -> output muon + Protonium channel
1s:2s
1s:2p
2s:2p
2p:1s
2p:2s
2p:2p

Table 1. Cross sections σ_{tr} and rates λ_{tr}, equation (41), for μ^- transfer reactions from a light hydrogen isotope to a heavier hydrogen isotope at low collision energies together with other theoretical results and experimental data. The result for unitarity ratio K_{21}/K_{12}, equation (37), are also presented for $\mathrm{t}+(\mathrm{d}\mu)_{1\mathrm{s}}$.

Energy		$\mathrm{t}+(\mathrm{d}\mu)_{1\mathrm{s}} \to (\mathrm{t}\mu)_{1\mathrm{s}}+\mathrm{d}$			$\mathrm{t}+(\mathrm{p}\mu)_{1\mathrm{s}} \to (\mathrm{t}\mu)_{1\mathrm{s}}+\mathrm{p}$		$\mathrm{d}+(\mathrm{p}\mu)_{1\mathrm{s}} \to (\mathrm{d}\mu)_{1\mathrm{s}}+\mathrm{p}$	
(eV)	Method	$\sigma_{\mathrm{tr}}/10^{-20}(\mathrm{cm}^2)$	$\lambda_{\mathrm{tr}}/10^8\ (\mathrm{s}^{-1})$	K_{21}/K_{12}	$\sigma_{\mathrm{tr}}/10^{-20}(\mathrm{cm}^2)$	$\lambda_{\mathrm{tr}}/10^8\ (\mathrm{s}^{-1})$	$\sigma_{\mathrm{tr}}/10^{-20}(\mathrm{cm}^2)$	$\lambda_{\mathrm{tr}}/10^8\ (\mathrm{s}^{-1})$
0.001	FH-type equations:	15.4	2.6	0.99	315.0	65.1	663.4	146.0
	[36]	15.8	2.7		384.4	80.0	828.7	170.0
	[37]	21.5	3.5		265.0	55.0	650.0	140.0
	[38]	18.0	2.8					
	[39]	14.2						
	Experiments:		2.8±0.5[58]			58.6±10[55]		84±13[54]
			2.8±0.3[57]					143±13[53]
			2.9±0.4[56]					95±34[52]
0.01	FH-type equations:	4.84	2.6	0.99	99.1	64.7	208.1	144.8
	[36]	5.64			128.0		283.7	
	[37]	4.8			60.0		140.0	
	[38]	5.0						
	[39]	4.44						
0.04	FH-type equations:	2.37	2.5	0.99	49.1	64.2	103.1	143.4
	[36]	2.94			63.6		140.7	
	[37]	3.1			40.0		91.0	
	[38]	2.5						
0.1	FH-type equations:	1.42	2.4	0.99	30.7	63.5	64.6	142.1
	[36]	2.0			39.9		87.4	
	[39]	1.35						

	$\bar{p} + (e^+e^-)_{1s} \rightarrow \bar{H} + e^-$		$\bar{p} + (\mu^+\mu^-)_{1s} \rightarrow \bar{H}_\mu + \mu^-$	
E (eV)	$\sigma_{\bar{H}}$ (cm^2)	$\sigma_{\bar{H}} v_{c.m.}$ (cm^3 s^{-1})	$\sigma_{\bar{H}_\mu}$ (cm^2)	$\sigma_{\bar{H}_\mu} v_{c.m.}$ (cm^3 s^{-1})
1.0e-06	0.16e-12	0.67e-08		
1.0e-05	0.50e-13	0.67e-08		
1.0e-04	0.16e-13	0.67e-08	0.18e-16	0.60e-12
1.0e-03	0.50e-14	0.66e-08	0.58e-17	0.60e-12
1.0e-02	0.15e-14	0.63e-08	0.18e-17	0.59e-12
5.0e-02	0.60e-15	0.56e-08	0.82e-18	0.59e-12
1.0e-01	0.42e-15	0.55e-08	0.58e-18	0.59e-12
5.0e-01			0.27e-18	0.62e-12
1.0e-00			0.23e-18	0.73e-12

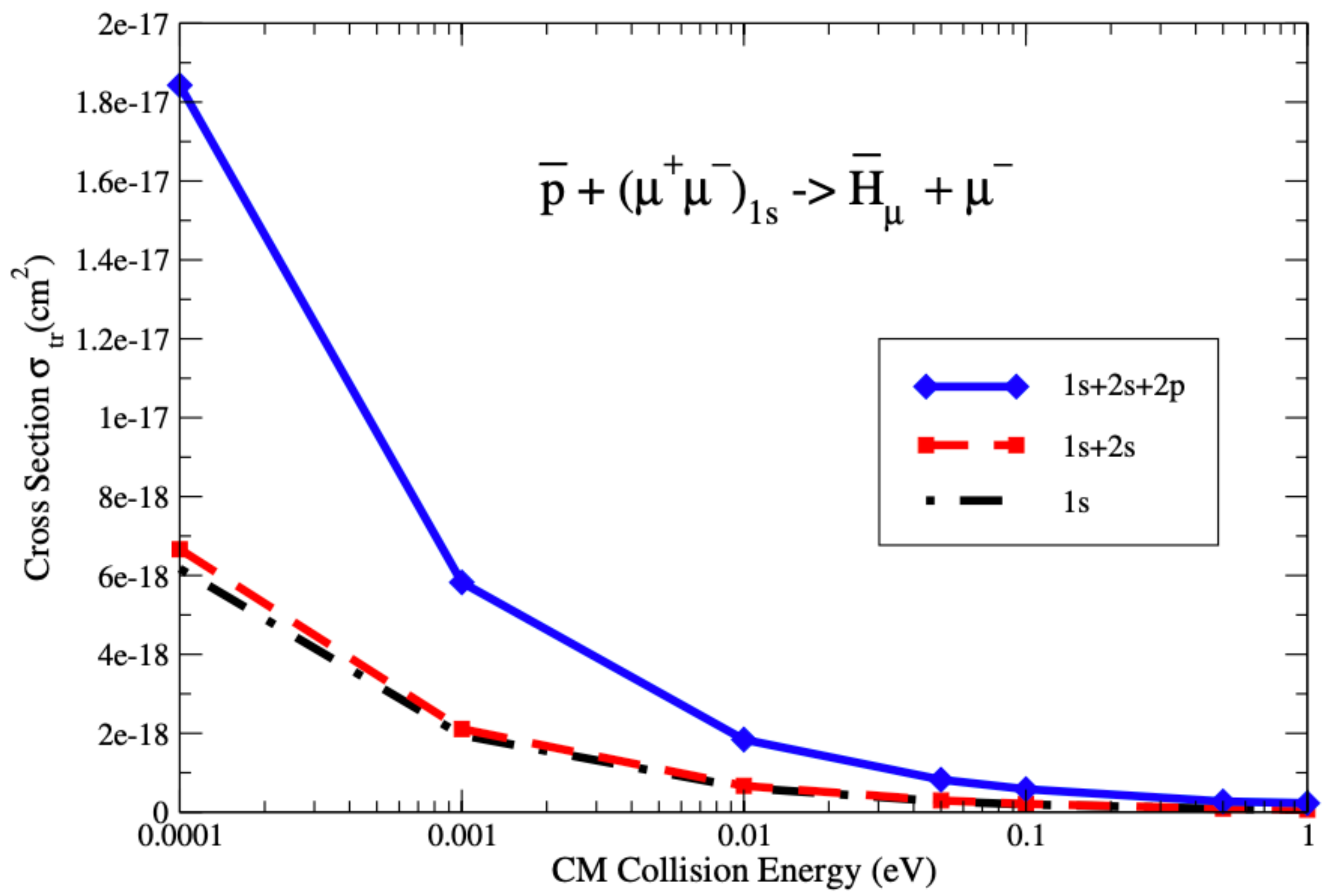

Figure 8. Low energy cross sections for a muonic antihydrogen formation reaction (2). Results are shown for the two-level 2×1s, four-level 2×(1s+2s), and six-level 2×(1s+2s+2p) close-coupling approximations.

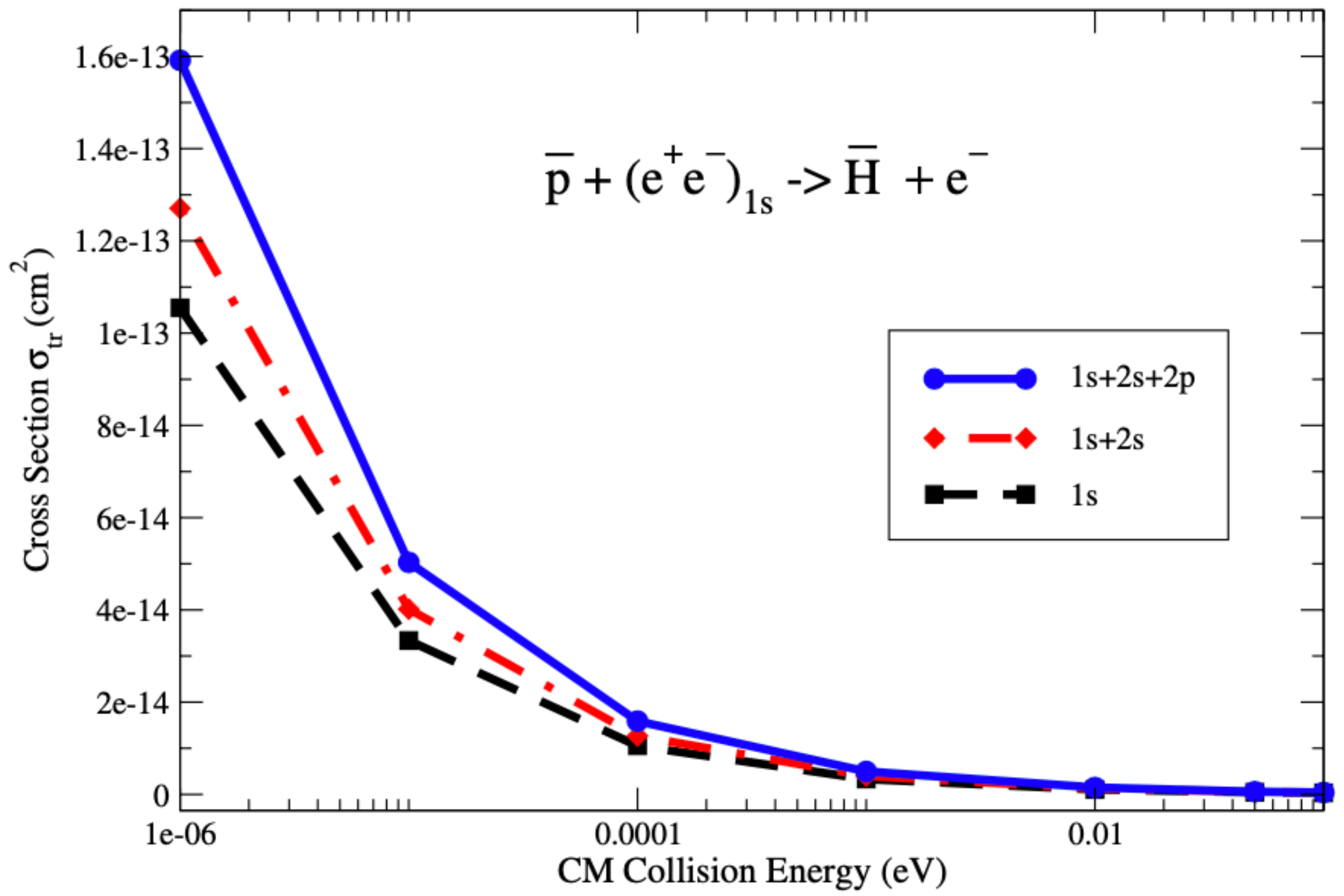

Figure 7. Low energy cross sections for an antihydrogen atom formation reaction (1). Results are shown for the two-level 2×1s, four-level 2×(1s+2s), and six-level 2×(1s+2s+2p) close-coupling approximations.

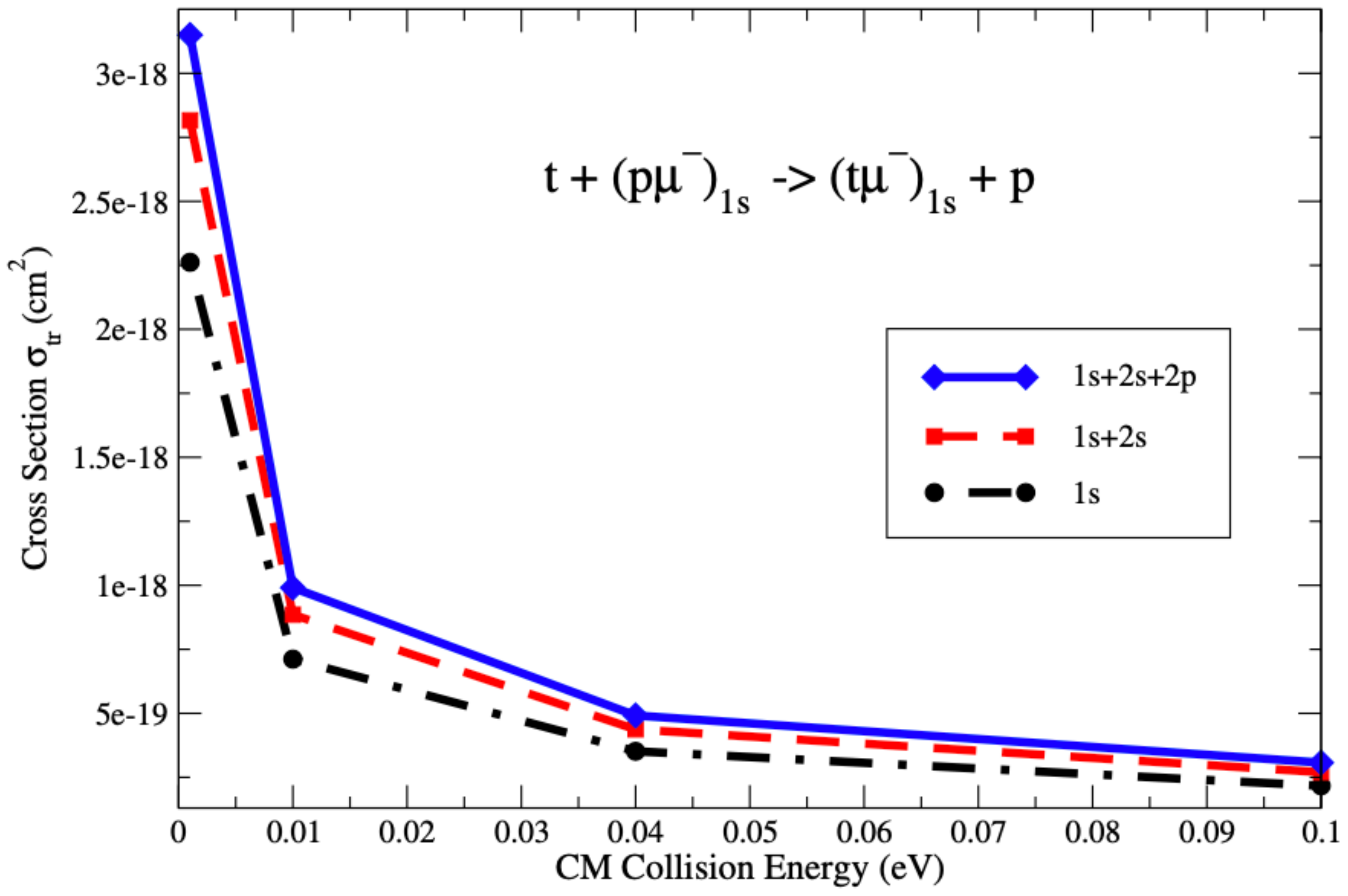

Figure 5. Low energy cross sections for a muon transfer reaction in the $t+(p\mu^-)_{1s}$ collision. Results are shown for the two-level $2\times1s$, four-level $2\times(1s+2s)$, and six-level $2\times(1s+2s+2p)$ close-coupling approximations.

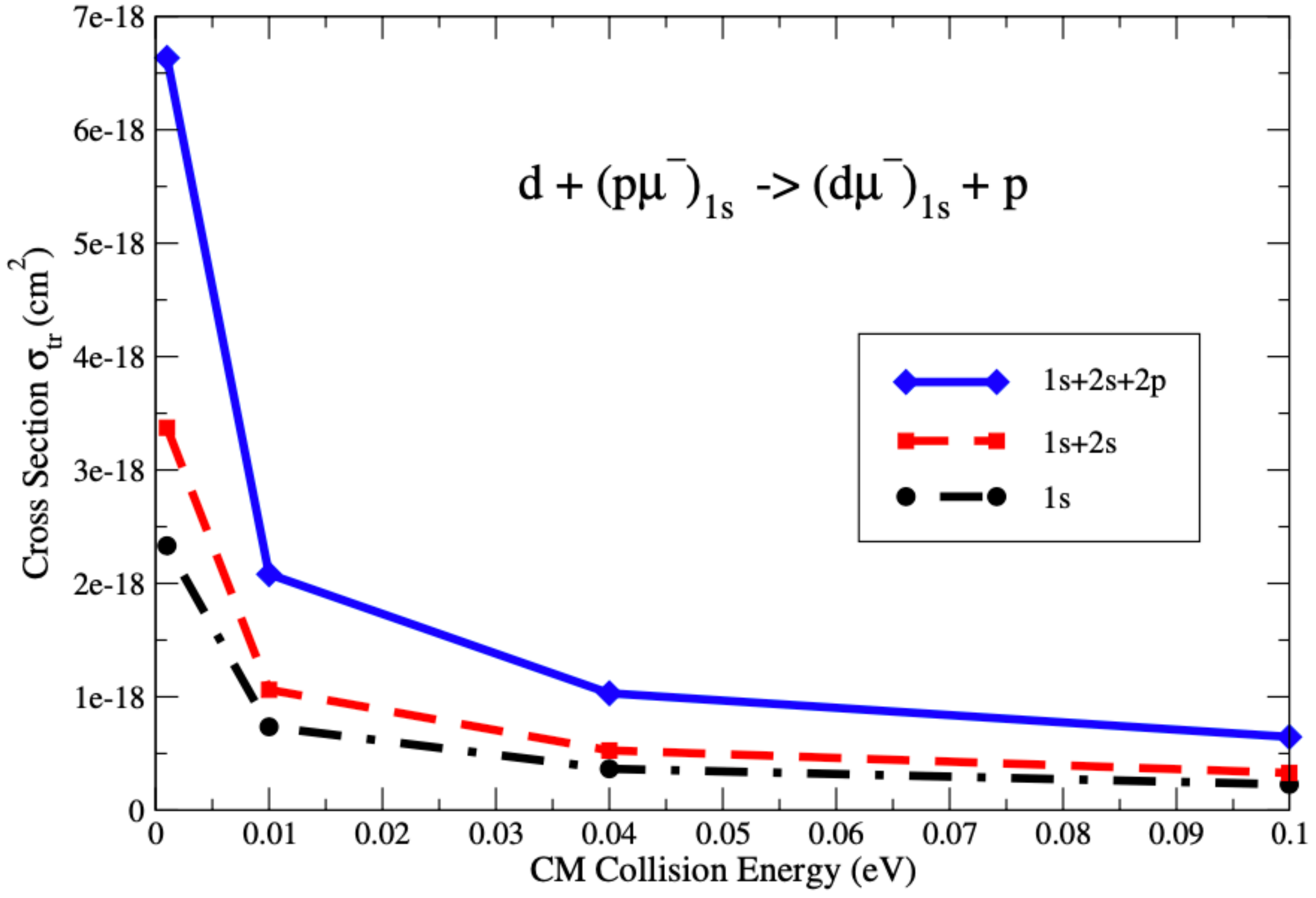

Figure 6. Low energy cross sections for a muon transfer reaction in the $d+(p\mu^-)_{1s}$ collision. Results are shown for the two-level $2\times1s$, four-level $2\times(1s+2s)$, and six-level $2\times(1s+2s+2p)$ close-coupling approximations.

Coulomb 3-Body Reactions With Strong Interaction in the Final State

- Reaction (1):
- $\bar{\mathrm{p}} + (\mathrm{D}\mu^-)_{1\mathrm{s}} \rightarrow (\bar{\mathrm{p}} - \mathrm{D})_{\mathrm{nl}} + \mu^-.$
- Reaction (2):
- $\bar{\mathrm{p}} + (\mathrm{T}\mu^-)_{1\mathrm{s}} \rightarrow (\bar{\mathrm{p}} - \mathrm{T})_{\mathrm{nl}} + \mu^-.$
- At low and very low-energy collisions $\varepsilon \sim 10^{-3}\ \mathrm{eV} - 3\ \mathrm{eV}$ the main contribution will be from the S-wave collision, i.e. the total orbital momentum in the 3-body system: L=0.
- Then $nl = 1s,\ 2s$ or $2\mathrm{p}$,
- We assume that other Coulomb atomic states maybe not important.
- In this calculations we consider only ground-state 1s to ground-state 1s reactions, i.e. $nl = 1s$.
- However, the nuclear forces are included in the final two-particle targets. To do this we appropriately shift the values of the pure Coulomb atomic levels.

RENAT A. SULTANOV, THE UNIVERSITY OF TEXAS PERMIAN BASIN, ODESSA TX USA (*SULTANOV_R@UTPB.EDU*)

Faddeev-Hahn Equations in Configuration Space:

- Two spatial configurations of three-charge-particle system:

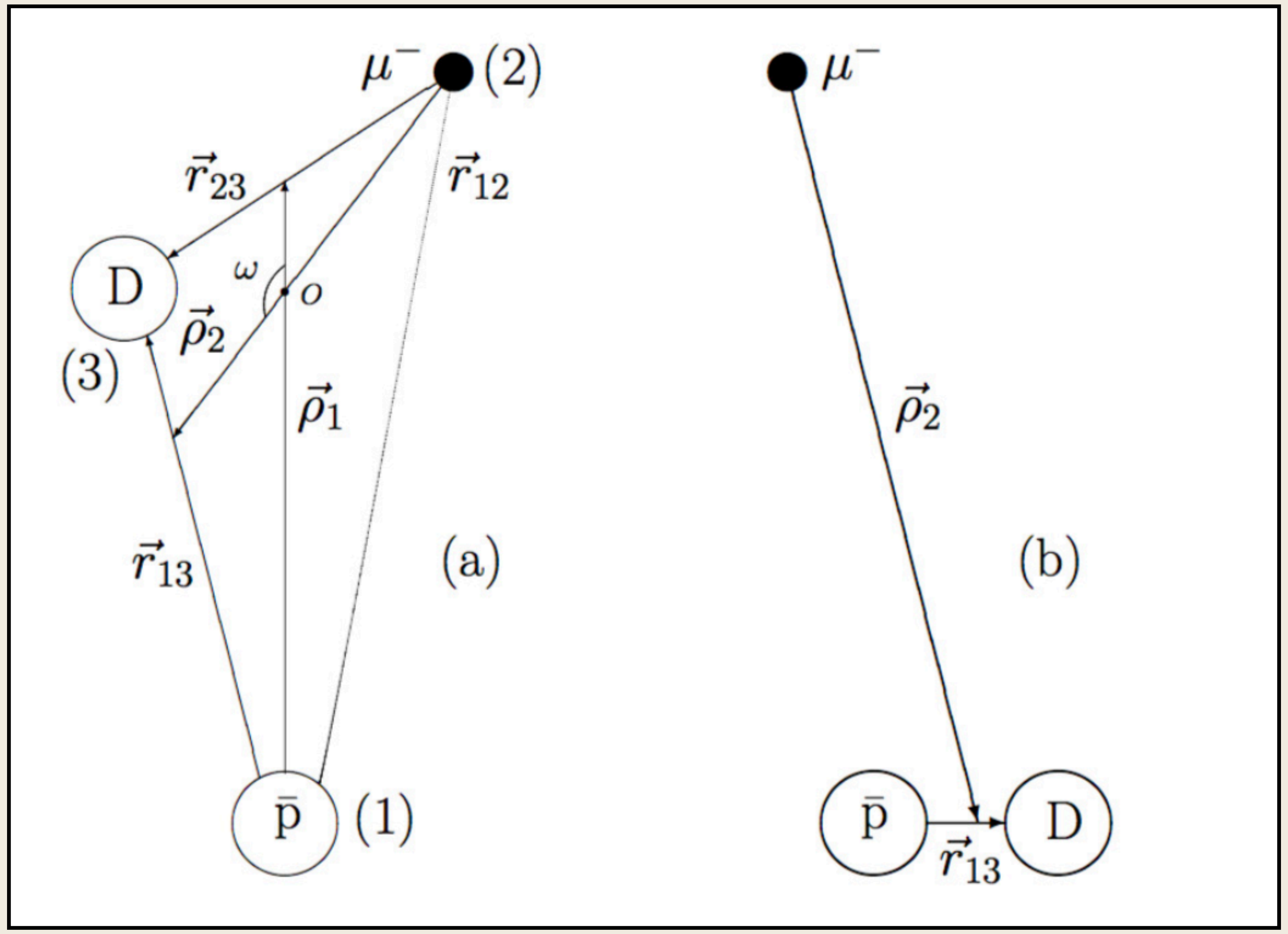

$$\Psi = \Psi_1(\vec{\rho}_1, \vec{r}_{23}) + \Psi_2(\vec{\rho}_2, \vec{r}_{13}).$$

$$\begin{aligned}\left(E - \hat{T}_{\rho_1} - \hat{h}_{23}(\vec{r}_{23})\right)\Psi_1(\vec{r}_{23}, \vec{\rho}_1) &= \left(V_{23}(\vec{r}_{23}) + V_{12}(\vec{r}_{12})\right)\Psi_2(\vec{r}_{13}, \vec{\rho}_2),\\ \left(E - \hat{T}_{\rho_2} - \hat{h}_{13}^{\bar{N}N}(\vec{r}_{13})\right)\Psi_2(\vec{r}_{13}, \vec{\rho}_2) &= \left(\tilde{\mathbf{V}}_{13}(\vec{r}_{13}) + V_{12}(\vec{r}_{12})\right)\Psi_1(\vec{r}_{23}, \vec{\rho}_1).\end{aligned}$$

$$\boxed{\tilde{\mathbf{V}}_{13}(\vec{r}_{13}) = V_{13}(\vec{r}_{13}) + v_{13}^{\bar{N}N}(\vec{r}_{13})}$$

Potentials and Target Hamiltonians

- Pair Coulomb potentials in the three-charge-particle systems+ nuclear interaction between hadrons: $\bar{p}-D$ and $\bar{p}-T$.
- Target hamiltonians:
- In the input channel:

$$\hat{h}_{23}(\vec{r}_{23}) = \hat{T}_{\vec{r}_{23}} + V_{23}(\vec{r}_{23})$$

- In the output channel:

$$\boxed{\hat{h}_{13}^{\bar{N}N}(\vec{r}_{13}) = \hat{T}_{\vec{r}_{13}} + V_{13}(\vec{r}_{13}) + v_{13}^{\bar{N}N}(\vec{r}_{13})}$$

- Modified Close-Coupling Approximation Approach is used: It leads to an expansion of the system's wave function components Ψ1 and Ψ2 into eigenfunctions of the subsystem (target) Hamiltonians:

$$\boxed{\begin{cases} \Psi_1(\vec{r}_{23}, \vec{\rho}_1) \approx \left(\int + \sum\right)_n f_n^{(1)}(\vec{\rho}_1)\varphi_n^{(1)}(\vec{r}_{23}), \\ \Psi_2(\vec{r}_{13}, \vec{\rho}_2) \approx \left(\int + \sum\right)_{n'} f_{n'}^{(2)}(\vec{\rho}_2)\varphi_{n'}^{(2)\bar{N}N}(\vec{r}_{13}). \end{cases}}$$

Modified Close-Coupling Approximation Approach

- This procedure brings a set of coupled one-dimensional integral-differential equations after the partial-wave projection.
- The set of coupled equations can be solved in the framework of different close-coupling approximations, such as 2×1s, 2×(1s+2s), 2×(1s+2s+2p) etc.
- The sign "2×" indicates that we use two independent sets of expansion functions.
- We consider Coulomb three-body systems with arbitrary masses, i.e. the masses of the charged particles are taken as they are.
- The final set of the equations is shown on the next slide:

Resulting Set of Coupled Equations:

$$\left[\left(k_n^{(1)}\right)^2+\frac{\partial^2}{\partial\rho_1^2}-\frac{\lambda(\lambda+1)}{\rho_1^2}\right]f_\alpha^{(1)}(\rho_1)=g_1\sum_{\alpha'}\frac{\sqrt{(2\lambda+1)(2\lambda'+1)}}{2L+1}\int_0^\infty \mathrm{d}\rho_2 f_{\alpha'}^{(2)}(\rho_2)$$
$$\times\int_0^\pi \mathrm{d}\omega\sin\omega R_{nl}^{(1)}(|\vec{r}_{23}|)\left[-\frac{1}{|\vec{r}_{23}|}+\frac{Z_1}{|\vec{r}_{12}|}\right]R_{n'l'}^{(2)}(|\vec{r}_{13}|)\rho_1\rho_2$$
$$\times\sum_{mm'}D_{mm'}^L(0,\omega,0)C_{\lambda 0lm}^{Lm}C_{\lambda'0l'm'}^{Lm'}Y_{lm}^*(\nu_1,\pi)Y_{l'm'}(\nu_2,\pi),$$

$$\left[\left(k_n^{(2)}\right)^2+\frac{\partial^2}{\partial\rho_2^2}-\frac{\lambda'(\lambda'+1)}{\rho_2^2}\right]f_\alpha^{(2)}(\rho_2)=g_2\sum_{\alpha'}\frac{\sqrt{(2\lambda+1)(2\lambda'+1)}}{2L+1}\int_0^\infty \mathrm{d}\rho_1 f_{\alpha'}^{(1)}(\rho_1)$$
$$\times\int_0^\pi \mathrm{d}\omega\sin\omega R_{nl}^{(2)}(|\vec{r}_{13}|)\left[-\frac{Z_1}{|\vec{r}_{13}|}+\frac{Z_1}{|\vec{r}_{12}|}\right]R_{n'l'}^{(1)}(|\vec{r}_{23}|)\rho_2\rho_1$$
$$\times\sum_{mm'}D_{mm'}^L(0,\omega,0)C_{\lambda 0lm}^{Lm}C_{\lambda'0l'm'}^{Lm'}Y_{lm}^*(\nu_2,\pi)Y_{l'm'}(\nu_1,\pi).$$

RAS et al., J. Comp. Phys. 192, 231-243 (2003)

Boundary Conditions and Cross Sections: K-matrix Formalism

$$\begin{cases} f_{1s}^{(1)}(\rho_1) \underset{\rho_1 \to +\infty}{\sim} \sin(k_1^{(1)}\rho_1) + K_{11}\cos(k_1^{(1)}\rho_1), \\ f_{1s}^{(2)}(\rho_2) \underset{\rho_2 \to +\infty}{\sim} \sqrt{v_1/v_2}K_{12}\cos(k_1^{(2)}\rho_2), \end{cases}$$

$$\begin{cases} f_{1s}^{(1)}(\rho_1) \underset{\rho_1 \to +\infty}{\sim} \sqrt{v_2/v_1}K_{21}\cos(k_1^{(1)}\rho_1), \\ f_{1s}^{(2)}(\rho_2) \underset{\rho_2 \to +\infty}{\sim} \sin(k_1^{(2)}\rho_2) + K_{22}\cos(k_1^{(2)}\rho_2), \end{cases}$$

$$\sigma_{ij} = \frac{4\pi}{k_1^{(i)2}} \left| \frac{\mathbf{K}}{1 - i\mathbf{K}} \right|^2 = \frac{4\pi}{k_1^{(i)2}} \frac{\delta_{ij} D^2 + K_{ij}^2}{(D-1)^2 + (K_{11} + K_{22})^2},$$

RAS et al., J. Phys. B 46, 215204 (2013)

How to Include Additional Nuclear Potential Between $\bar{\mathrm{p}}$-D and $\bar{\mathrm{p}}$-T ?

- Low-energy reaction (1):
  $\bar{\mathrm{p}} + (\mathrm{D}\mu^-)_{1s} \to (\bar{\mathrm{p}} - \mathrm{D})_{1s} + \mu^-$.
- Low-energy reaction (2):
  $\bar{\mathrm{p}} + (\mathrm{T}\mu^-)_{1s} \to (\bar{\mathrm{p}} - \mathrm{T})_{1s} + \mu^-$.
- The full potentials between $\bar{\mathrm{p}}-\mathrm{D}$ and $\bar{\mathrm{p}}-\mathrm{T}$ are more complex, because their second parts possess asymmetric nuclear interactions.
- In this work we do not explicitly include the strong interaction in calculations.

- Which is why in the case of the target $(\bar{\mathrm{p}}-\mathrm{D})$ and $(\bar{\mathrm{p}}-\mathrm{T})$ eigenfunctions we use only pure Coulomb 2-body-atomic wave-functions.
- Nonetheless, the strong nuclear interactions are approximately taken into account:
- through the eigenstates $\mathcal{E}_{n'}$ which have shifted values from the Coulomb levels (original), i.e. $\varepsilon_{n'}$.

Inclusion of the Strong Interaction:

$$\varphi_{n'}^{(2)\bar{N}N}(\vec{r}_{13}) \approx \sum_{l'm'} R_{n'l'}^{(2)\bar{N}N}(r_{13}) Y_{l'm'}(\vec{r}_{13}) \approx \sum_{l'm'} R_{n'l'}^{(2)}(r_{13}) Y_{l'm'}(\vec{r}_{13})$$

$$\mathcal{E}_{n'} \approx \varepsilon_{n'} + \Delta E_{n'}^{\bar{N}N} = -\mu_2/2n'^2 + \Delta E_{n'}^{\bar{N}N}$$

$$\Delta E_{n'}^{\bar{N}N} = -\frac{4}{n'} \frac{a_s}{B_{\bar{\mathrm{p}}\mathrm{H}}} \varepsilon_{n'}$$

S. Deser, M. L. Goldberger, K. Baumann, and W. Thirring, Phys. Rev. 96, 774 (1954)

Parameters of the p̄-D strong interaction

- For calculations of the energy shifts in the (p̄p) atom a special Deser-Goldberger-Baumann-Thirring formula has been used in these calculations.
- $R_{1s}(Pn)$ ~ 60 fm; $E_{1s}(Pn)$~12 keV,
- $R_{1s}(p\mu)$~285 fm ; $E_{1s}(p\mu)$~2.5 кeV.
- p̄ + p scattering length: **A_0 = 0.57 fm**
- **$\Delta E_{1s}(Pn)$ = 494 eV; $\Delta E_{2s}(Pn)$ = 62 eV.**

- RAS et al., Atoms 6(2), 18 (2018) (MDPI)

- Parameters for (p̄D):
- **ΔE_{1s}(p̄D) = 1050 eV; ΔE_{2s}(p̄D) = 131.25 eV.**
- p̄+D scattering length: **A_0 = 0.682 fm**
- Parameters for (p̄T):
- **ΔE_{1s}(p̄T) = 1575 eV.**
- **This is a rough approximation (model).**
- In the literature no results for (p̄T) atomic Coulomb energy level shifts or p̄+T scattering length.

Results for cross sections: $\bar{\mathrm{p}} + \mathrm{D}\mu$

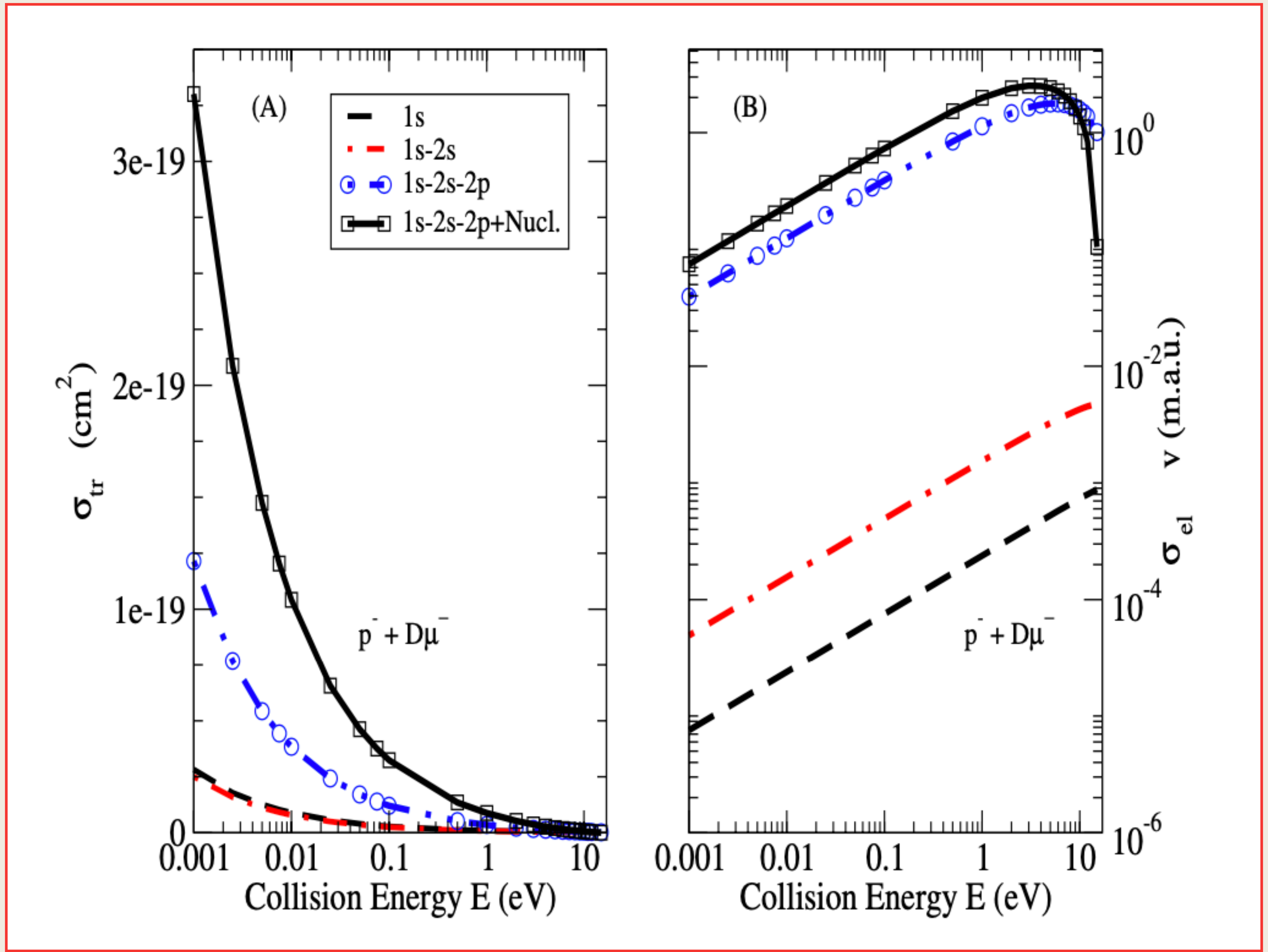

Results for cross sections: $\bar{p} + T\mu$

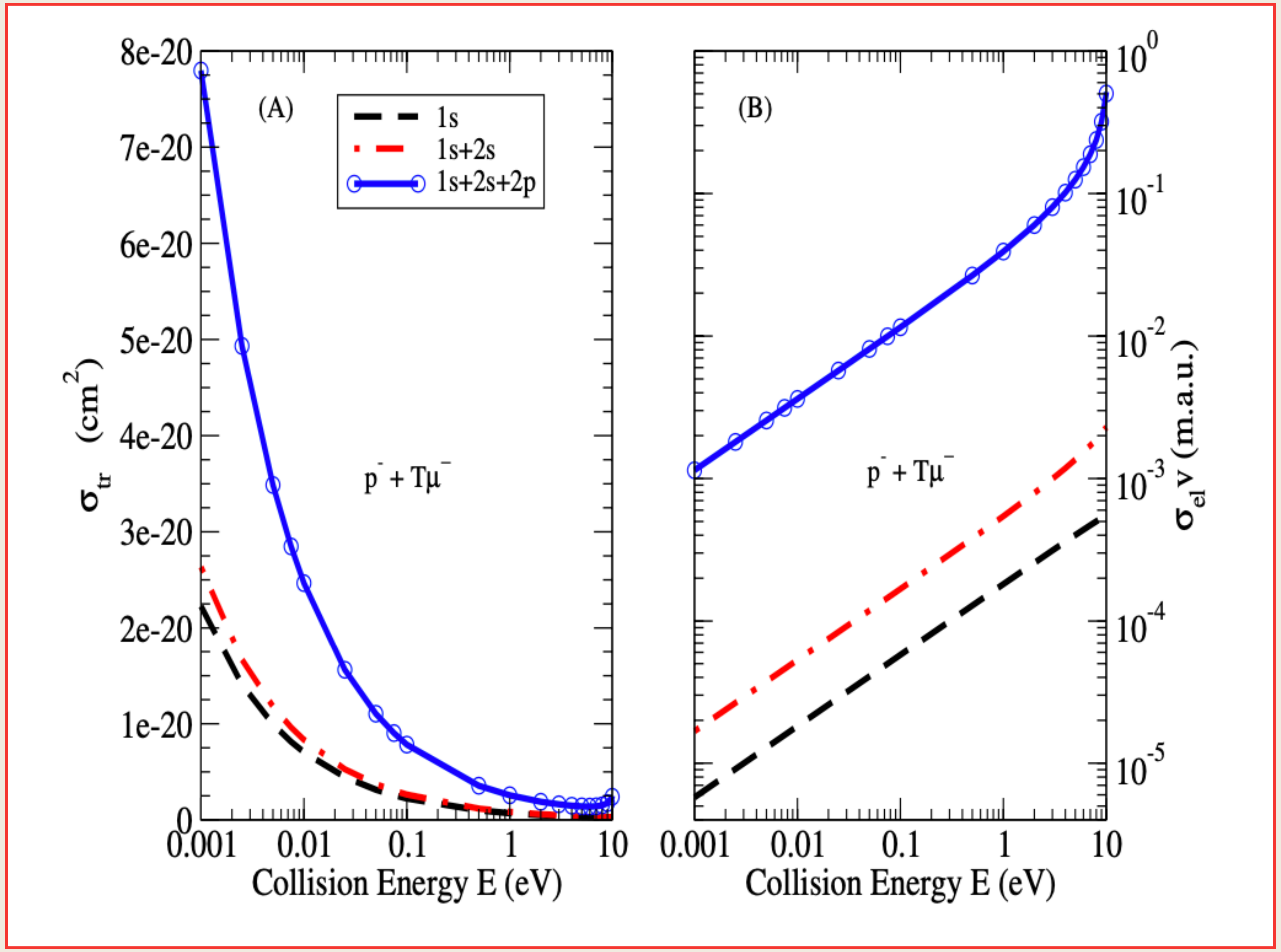

Results for reaction rates: $\bar{\mathrm{p}} + \mathrm{D}\mu$ & $\bar{\mathrm{p}} + \mathrm{T}\mu$

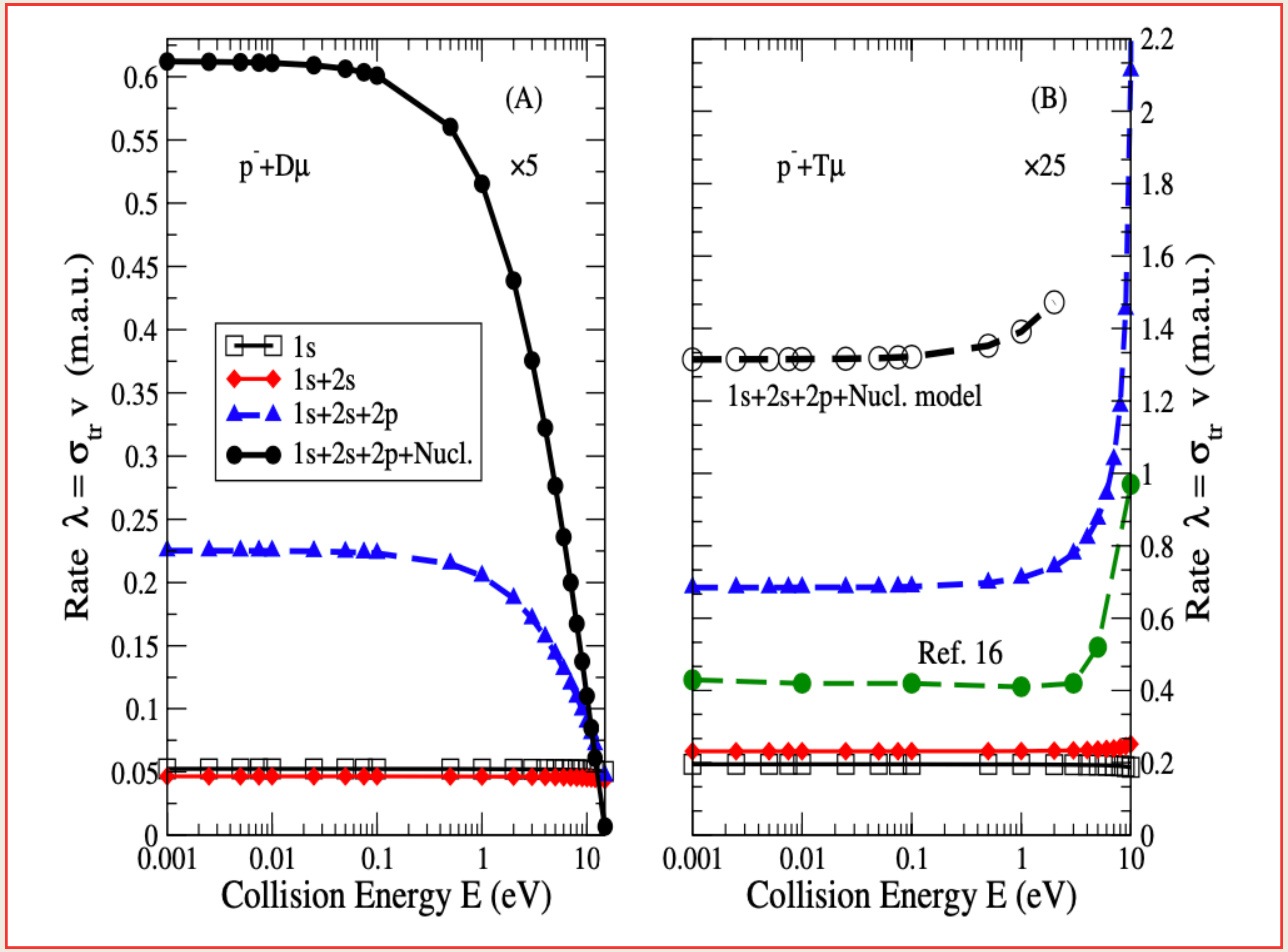

Ref. 16: Igarashi, N. Toshima, Eur. Phys. J. D 46, 425 (2008)

Conclusions

- The 3-body $\bar{\mathrm{p}} + (\mathrm{D}\mu^-)$ and $\bar{\mathrm{p}} + (\mathrm{T}\mu^-)$ reactions have been computed in the framework of a detailed few-body approach.
- Two-component Faddeev-Hahn-type equations have been used within a modified close-coupling expansion techniques: 2X(1s+2s+2p) - 6 state approximation.
- Approximate inclusion of the strong interaction in the final states **increased dramatically the results** for the ($\bar{\mathrm{p}}$D) and ($\bar{\mathrm{p}}$T) antiprotonic hydrogen atom formation reaction cross sections and rates.
- We assume (believe) that the 3-body antiprotonic/muonic reactions can be used for further study of the $\bar{\mathrm{p}}$-D and $\bar{\mathrm{p}}$-T nuclear interactions and potentials.

Future Plans: (I) Few-Body Systems in μCF

TABLE I. Low-energy s-wave $d + (t\mu^-)_{1s}$ elastic scattering results for $K_{11} = \tan(\delta(\varepsilon_c))$ together with the results of works [67] and [68] at kinetic energy ε_c below the $(t\mu^-)_{n=2}$ threshold.

ε_c (eV)	This work	Ref. [67]	Ref. [68]
0.01	−0.0247	−0.02384	
0.04	−0.0494	−0.0509	
0.1	−0.0784	−0.0856	−0.0875
0.3	−0.1360	−0.1627	
0.5	−0.1761	−0.2206	−0.220
1.0	−0.2509	−0.3363	−0.335

[67] C. Chiccoli *et al*., Muon Catalyzed Fusion **7**, 87 (1992).
[68] A. A. Kvitsinsky, C.-Y. Hu, and J. S. Cohen, Phys. Rev. A **53**, 255 (1996).

RAS et al., Phys.Rev. C 107, 064003 (2023)

$$(t\mu^-)_{1s} + d \to d + (t\mu^-)_{1s}$$

$$f_{\alpha}^{(1)}(\rho_1) \underset{\rho_1\to 0}{\sim} f_{\alpha'}^{(2)}(\rho_2) \underset{\rho_2\to 0}{\sim} 0.$$

$$f_{1s}^{(1)}(\rho_1) \underset{\rho_1\to+\infty}{\sim} \sin\left(k_{n=1}^{(1)}\rho_1\right) + K_{11}\cos\left(k_{n=1}^{(1)}\rho_1\right),$$
$$f_{\alpha'}^{(2)}(\rho_2) \underset{\rho_2\to+\infty}{\sim} 0.$$

$$(t\mu^-)_{1s} + D_2 \to [(dt\mu^-)^*_{L=1}de^-] + e^-$$

Future Plans: (II) 3-Body Systems with X^-

$$d + (pX^-) \rightarrow (pX^-) + d$$
$$\searrow (dX^-) + p, \qquad (2)$$

RAS et al., Phys.Rev. C 107, 064003 (2023)

(X^-: **tau slepton or stau**)

TABLE II. Reaction channel total cross sections σ_t and rates λ in collision (2) at very low energies together with the corresponding results of work [10] obtained under different quantum-mechanical approximations. Here ε_c is the collision energy, v is the center-of-mass collision velocity, $\pi a_p^2 = 26.1$ b, $a_p = 28.8$ fm is the (pX^-) Bohr radius, and $\lambda = N_0 \sigma_t v$, where $N_0 = 4.25 \times 10^{22}$ cm^3 is the hydrogen density.

This work					Results from Ref. [10]		
ε_c (eV)	v (km/s)	σ_t (units of πa_p^2)	σ_t (cm^2)	λ (s^{-1})	λ^a (s^{-1})	λ^b (s^{-1})	λ^c (s^{-1})
0.0001	0.0988	4.135×10^4	107.91×10^{-20}	4.53×10^8	$\approx 0.3 \times 10^8$	$\approx 1.8 \times 10^8$	$\approx 12 \times 10^8$
0.001	0.312	1.307×10^4	34.11×10^{-20}	4.53×10^8			
0.01	0.988	0.413×10^4	10.77×10^{-20}	4.52×10^8			
0.1	3.12	1.30×10^3	3.38×10^{-20}	4.48×10^8			

[a] Screened potential approximation.
[b] Screened+dipole.
[c] Three-body Born.

[10] Sawicki, M. Gajda, D. Harley, and J. Rafelski, Phys. Rev **44**, 4345 (1991).

"Nuclear fusion catalyzed by doubly charged scalars: Implications for energy production", by E Ahmedov, Phys. Rev. D **106**, 035013 (2022)

Thank You!